

# PQCache: Product Quantization-based KVCache for Long Context LLM Inference

HAILIN ZHANG\*, Peking University, China

XIAODONG JI\*, Peking University, China

YILIN CHEN\*, Peking University, China

FANGCHENG FU\*, Peking University, China

XUPENG MIAO, Purdue University, USA

XIAONAN NIE\*, Peking University, China

WEIPENG CHEN, Baichuan Inc., China

BIN CUI\*<sup>†</sup>, Peking University, China

As the field of Large Language Models (LLMs) continues to evolve, the context length in inference is steadily growing. Key-Value Cache (KVCache), the intermediate representations of tokens within LLM inference, has now become the primary memory bottleneck due to limited GPU memory. Current methods selectively determine suitable keys and values for self-attention computation in LLMs to address the issue. However, they either fall short in maintaining model quality or result in high serving latency. Drawing inspiration from advanced embedding retrieval techniques prevalent in the data management community, we consider the storage and retrieval of KVCache as a typical embedding retrieval problem. We propose **PQCache**, which employs Product Quantization (PQ) to manage KVCache, maintaining model quality while ensuring low serving latency. During the prefilling phase, we apply PQ to tokens' keys for each LLM layer and head. During the autoregressive decoding phase, we use PQ codes and centroids to approximately identify important preceding tokens, then fetch the corresponding key-value pairs for self-attention computation. Through meticulous design of overlapping and caching, we minimize any additional computation and communication overhead during both phases. Extensive experiments demonstrate that PQCache achieves both effectiveness and efficiency, with 4.60% score improvement over existing methods on InfiniteBench and low system latency in both prefilling and decoding.

CCS Concepts: • **Computing methodologies** → **Artificial intelligence**; • **Information systems** → **Information retrieval**.

Additional Key Words and Phrases: Large Language Model, Long Context Inference, KVCache Management, Information Retrieval, Product Quantization

\*Hailin Zhang, Xiaodong Ji, Yilin Chen, Fangcheng Fu, Xiaonan Nie, and Bin Cui are with the School of Computer Science & Key Lab of High Confidence Software Technologies (MOE), Peking University. Bin Cui is also with the Institute of Computational Social Science, Peking University (Qingdao).

<sup>†</sup>Bin Cui is the corresponding author.

Authors' Contact Information: Hailin Zhang, z.hl@pku.edu.cn, Peking University, China; Xiaodong Ji, xiaodong.0731@stu.pku.edu.cn, Peking University, China; Yilin Chen, yilinoology@gmail.com, Peking University, China; Fangcheng Fu, ccchengff@pku.edu.cn, Peking University, China; Xupeng Miao, xupeng@purdue.edu, Purdue University, USA; Xiaonan Nie, xiaonan.nie@pku.edu.cn, Peking University, China; Weipeng Chen, hitesgavin@gmail.com, Baichuan Inc., China; Bin Cui, bin.cui@pku.edu.cn, Peking University, China.

Permission to make digital or hard copies of all or part of this work for personal or classroom use is granted without fee provided that copies are not made or distributed for profit or commercial advantage and that copies bear this notice and the full citation on the first page. Copyrights for components of this work owned by others than the author(s) must be honored. Abstracting with credit is permitted. To copy otherwise, or republish, to post on servers or to redistribute to lists, requires prior specific permission and/or a fee. Request permissions from [permissions@acm.org](mailto:permissions@acm.org).

© 2025 Copyright held by the owner/author(s). Publication rights licensed to ACM.

ACM 2836-6573/2025/6-ART201

<https://doi.org/10.1145/3725338>

## ACM Reference Format:

Hailin Zhang, Xiaodong Ji, Yilin Chen, Fangcheng Fu, Xupeng Miao, Xiaonan Nie, Weipeng Chen, and Bin Cui. 2025. PQCache: Product Quantization-based KVCache for Long Context LLM Inference. *Proc. ACM Manag. Data* 3, 3 (SIGMOD), Article 201 (June 2025), 30 pages. <https://doi.org/10.1145/3725338>

## 1 Introduction

Large Language Models (LLMs), such as GPT [69] and Llama [26], have demonstrated exceptional performance in the task of “next token prediction”, which encompasses a broad range of applications in text understanding and generation [26, 39, 53, 98, 103]. Beyond their extensive applications in language processing, transformer-based LLMs have also been successfully utilized in multi-modal contexts, including image analysis [25, 72], video processing [80], software-engineering [18, 39, 109], databases [117, 118], and scientific AI applications [4, 12]. In recent years, the maximum input length of LLM inference has seen a substantial increase, in order to achieve better model performance through in-context learning [13, 65, 83], as well as to enable various complicated applications across different domains [15, 67, 94, 114]. The maximum input length has grown from 2K-4K [86, 88] to 32K [45, 87], 128K [26, 30, 69], and even millions of tokens [3, 20, 55].

During inference, LLMs takes a sequence of tokens (also referred to as the context) as input and autoregressively generates subsequent tokens. A typical LLM employs decoder-only self-attention modules to facilitate interaction between tokens. Each module calculates the “query”, “key”, and “value” representations for each token, multiplies queries and keys, and uses the softmax function to derive attention scores. These scores are then used for weighted summation of the values. As a decoder-only model, the query of each token can only access the keys and values of preceding tokens. Therefore, the keys and values of previous tokens are utilized for subsequent tokens, while newly generated tokens do not influence previous ones. The LLM inference process consists of one *prefilling* phase and multiple *decoding* phases. In each phase, the LLM generates a new token. During prefilling, the LLM processes the lengthy input and compute keys and values for all input tokens. During each decoding phase, to avoid redundant computations, the LLM only processes the last generated token and produces its key and value. Preceding tokens’ keys and values, referred to as the Key-Value Cache (KVCache), are saved and reused by later tokens. More details about LLM inference can be found in Section 2.1.

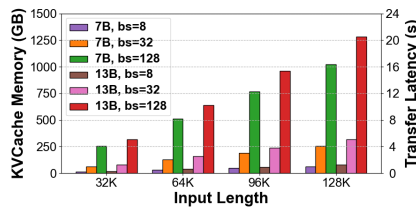


Fig. 1. KVCache memory size and theoretical CPU-GPU transfer latency over PCI-e Gen 5 for varying batch sizes (bs), model sizes (7B and 13B), and sequence lengths.

As sequence lengths continue to grow in nowadays applications, the memory consumption of KVCache has increased dramatically, far exceeding the memory capacity of individual GPUs. For instance, using a 7B model for inference on 128K-length sequences, a batch of 128 samples requires 1TB of KVCache memory as shown in Figure 1, which surpasses the 640GB GPU memory available in an 8-card A100 setup. In such cases, the KVCache needs to be stored in lower-level memory hierarchies, resulting in time-consuming transfer latency and complex scheduling [58, 81, 84], which hinders normal generation process. Essentially, the task of managing large-scale KVCache

within constrained GPU memory, while optimizing both model quality and efficiency, is a data management problem.

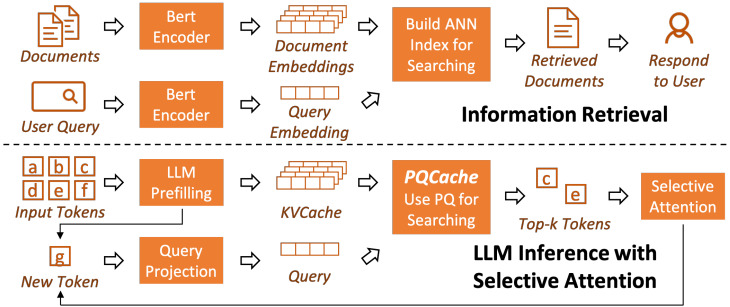


Fig. 2. Comparison between information retrieval and LLM inference with selective attention.

To address the memory challenge posed by KVCache in long-context LLM inference, a natural solution is *selective attention* [64], which incorporates only relevant tokens for attention computation, rather than using all previous tokens. This solution is based on the observation that, during each step of generation, certain tokens significantly influence the outcome, as their attention scores are considerably larger than others [59, 112]. This finding is also corroborated in Section 3.1. Building on the concept of selective attention, numerous methods have been proposed, broadly classified into two categories: KVCache dropping [59, 100, 112] and KVCache offloading [79, 99]. However, existing methods fail to achieve effectiveness and efficiency simultaneously, as they either rely on improper assumptions or introduce notable latency.

KVCache dropping methods discard key-value pairs deemed unimportant in earlier steps, assuming that these tokens will not affect subsequent generation. However, the assumption often fails in real-world tasks, as tokens with initially low weights may gain importance in later steps and influence subsequent outputs [23, 50, 102]. Existing KVCache offloading methods, including SPARQ [79] and InfLLM [99], store the entire KVCache on CPU. For each newly generated token, they fetch relevant key-value pairs based on low-cost proxy scores. SPARQ identifies a subset of dimensions with large magnitude in queries, fetches only these dimensions from all keys, and computes inner-product to determine the most relevant tokens. Despite its effectiveness, SPARQ incurs substantial communication overhead that cannot be overlapped with computations. InfLLM organizes the KVCache into blocks and uses representative tokens from each block to compute relevance. Though the block-level space-continuity assumption improves efficiency, it does not align with real scenarios where relevant tokens are distributed discretely, leading to a significant drop in model quality. In summary, existing methods fall short in achieving both effectiveness and efficiency for long-context LLM inference.

We observe that selective attention is essentially an information retrieval process, as it requires to find the top- $k$  relevant tokens' key-value pairs based on query-key multiplications. Information retrieval, a prevalent research area within the database and data management domains, encompasses many well-known methods including Product Quantization [5, 27, 32, 34, 44, 57, 91], inverted index [11, 16, 96, 104, 116], and graph-based methods [7, 8, 43, 61, 62, 113]. As shown in Figure 2, information retrieval typically involves two phases: (1) index construction, where document embedding vectors are generated by an encoder and organized into an Approximate Nearest Neighbor (ANN) index; (2) searching, which aims to efficiently retrieve the top- $k$  relevant embedding vectors from the index for a given query embedding. Interestingly, the selective attention process in LLM

inference aligns with these phases of information retrieval. During the prefilling phase, the input tokens' KVCache is generated, with the keys serving as the embedding vectors for index construction. Then, the decoding phase retrieves relevant tokens given the new token's query embedding vector, which corresponds to the searching phase in information retrieval.

Drawing inspiration from the field of information retrieval, we propose **PQCache**, a novel approach that integrates retrieval techniques into the management of KVCache to ensure both effectiveness and efficiency in long-context LLM inference. During the prefilling phase, we generate the KVCache, store it in CPU memory, and then construct index structures. In the decoding phase, we efficiently retrieve relevant key-value pairs using the constructed index. Given the latency requirements of LLM inference, we do not consider methods with expensive index construction overheads, such as graph-based methods or complex inverted-index methods. Instead, we leverage the low-cost Product Quantization (PQ) technique [44], which partitions embeddings into sub-embeddings then conducts clustering.

The core concept of PQCache involves constructing PQ structures using preceding token keys and performing efficient searching to retrieve relevant key-value pairs for subsequent self-attention computations. PQ provides a well-behaved approximation of embedding vectors (and their inner product), while consuming only a small amount of memory. During the prefilling phase, we apply PQ to the generated keys for each layer and head, resulting in PQ codes and centroids through clustering on CPU. At each autoregressive decoding step, we perform inner product between the partitioned query and the PQ centroids, then combine with PQ codes to obtain the approximate attention weights. Using the approximation, we retrieve top- $k$  relevant key-value pairs from CPU memory for self-attention computation, eliminating the need to access the entire KVCache. To further facilitate efficient LLM inference, we leverage system optimization opportunities to reduce latency. We implement prefetching and overlapping wherever possible: KVCache offloading, PQ construction, and the fetching of PQ codes are overlapped with LLM computation. To maximize GPU memory utilization and minimize CPU-GPU communication, we introduce a block-level cache on GPU specifically for frequently accessed key-value pairs. Further experimental analysis show that PQCache improves the InfiniteBench scores by 4.60% compared to existing methods, while maintaining low system latency.

To the best of our knowledge, this is the first work that incorporates information retrieval techniques to address the KVCache memory challenge. Information retrieval, aimed at identifying relevant information from vast resources, is a critical component of modern web services. As a burgeoning application, long-context LLM inference also deals with a large volume of information within the representation of the input context. Therefore, our innovative approach of integrating retrieval techniques into LLM inference presents an intuitive and effective solution. With the proposal of PQCache, we are not only addressing a current challenge but also pioneering a new domain for efficient LLM inference. Looking ahead, we anticipate that this integration will become a standard paradigm in next-generation LLM inference, propelling the field forward and establishing a significant milestone for efficiency and effectiveness.

We summarize our contributions as follows:

- We effectively implement the information retrieval technique PQ into KVCache management, enhancing both model performance and efficiency of LLM inference.
- We propose a system-algorithm co-designed approach PQCache to approximately retrieve the top- $k$  relevant keys for a given query, with meticulous design of overlapping and caching.
- We evaluate PQCache through extensive experiments. It improves the InfiniteBench scores by 4.60% compared to existing methods, while achieving low system latency.

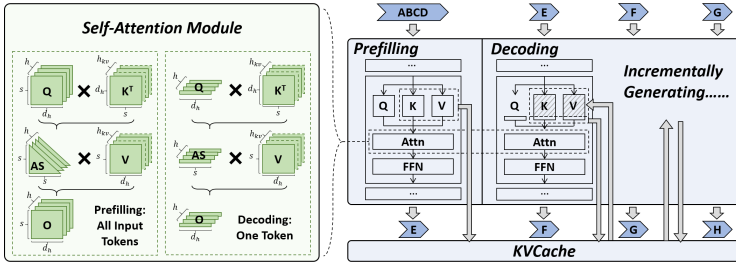


Fig. 3. An overview of LLM inference. The left part illustrates the computation process of the self-attention module, where “Q”, “K”, “V”, “AS”, and “O” represent query, key, value, attention score, and output, respectively. The right part depicts the LLM inference process, consisting of the prefilling phase and the decoding phase, where “Attn” and “FFN” represent the attention layer and the feed-forward network layer, respectively. The mathematical symbols are detailed in Table 1.

Table 1. Notations. “#” means “the number of”.

Sym.	Explanation	Sym.	Explanation
$n$	Batch size.	$m$	# partitions in PQ.
$s$	Current sequence length.	$b$	# bits for PQ codes.
$d$	Hidden states dimension.	$d_m$	Dimension of each partition.
$h_{(kv)}$	# heads (for keys and values).	$k$	# tokens in selective attention.
$d_h$	Dimension of each head.	$T$	# K-Means iterations.

## 2 Preliminary

In this section, we introduce fundamental concepts related to LLM, PQ, and the memory hierarchy.

### 2.1 Large Language Model Inference

An overview of LLM inference is depicted in Figure 3. An LLM consists of a vocabulary embedding for input, a stack of transformer layers, and a token classifier for output. The self-attention module, which is a crucial component of a transformer layer, facilitates interaction and information aggregation among different tokens. Following the notations in Table 1, each transformer layer receives an input of shape  $(n, s, d)$ . The input is separately projected and transposed for query, key, value, resulting in the same shape of  $(n, h, s, d_h)$ , where it usually holds that  $d = h * d_h$ . Different heads are expected to capture different semantic information. The attention mechanism multiplies the queries and keys, applies a lower-triangular causal mask to restrict queries to preceding keys only, and performs softmax to obtain the attention scores of shape  $(n, h, s, s)$ . The attention scores are then used to weighted-sum the values, yielding an output of shape  $(n, h, s, d_h)$ . In long-context inference, the  $O(s^2)$  space complexity associated with operations among queries, keys, and values is impractical. Consequently, modern LLMs typically employ FlashAttention [21, 22], which utilizes tiled matrix multiplication and softmax, to only use  $O(s)$  space complexity for attention computation. It’s worth noting that, the time complexity of attention computation remains  $O(s^2)$ . The output from attention is later reshaped into  $(n, s, d)$  for the subsequent fully-connected layers, also known as Feed-Forward Network (FFN). To alleviate memory and computation burden, Grouped-Query Attention (GQA) is often applied. It employs a smaller number of heads  $h_{kv}$  for keys and values, resulting in their shape being  $(n, h_{kv}, s, d_h)$ . In this setup, each key-value pair corresponds to multiple queries.

During LLM inference, each execution of the model generates a new token, following an autoregressive manner. The first traversal of the LLM is called “prefilling”, and subsequent traversals are referred to as “decoding”, as shown in Figure 3. In the prefilling phase, the self-attention module computes the queries, keys, and values for all input tokens, and stores the key-value pairs as KVCache for later use. Thanks to the causal mask, later tokens do not affect earlier tokens, so in the autoregressive decoding phase we only need to compute the query, key, value for the last generated token. This process leverages previous keys and values from the KVCache, and computes an attention score of shape  $(n, h, 1, s)$ . Concurrently, the newly generated key and value are added to the KVCache. As a result, the memory consumption of KVCache scales linearly with the sequence length, leading to a memory bottleneck in scenarios involving long-context input and output.

## 2.2 Product Quantization

PQ [44] was proposed to facilitate efficient Approximate Nearest Neighbor Search (ANNS), retrieving relevant embedding vectors from a large pool of candidates given a query embedding vector. As shown in Figure 4, PQ involves two phases: index construction and searching. During construction, PQ divides each candidate embedding into  $m$  partitions, essentially decomposing the original embedding space into  $m$  separate sub-spaces. Each sub-space undergoes K-Means clustering to group the sub-embeddings, yielding  $2^b$  centroids. Each embedding is then assigned  $m$  codes, each with  $b$  bits, indicating the centroids it belongs to. These compact PQ codes enable the reconstruction of approximate embeddings using centroids, significantly reducing memory requirements. During searching, the query embedding is divided into  $m$  partitions. Similarity is computed with the centroids within each partition, and aggregated through PQ codes, bypassing the need for full similarity calculations with every embedding.

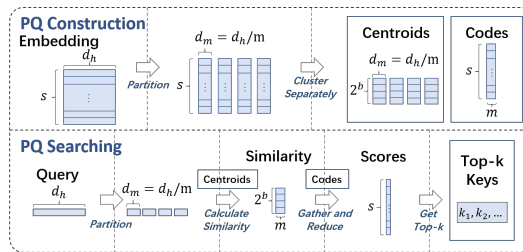


Fig. 4. An overview of PQ construction and searching.

PQ has a profound impact on ANNS, with its principles integrated into various efficient ANNS methods [11, 43, 48]. While PQ was initially designed together with IVF (inverted file system) [44] for ANNS, PQ and IVF are independent techniques and are often applied separately [34, 48, 101]. PQ’s variants are also applied in various learning tasks [54, 89, 108] to achieve effective compression and efficient computation. In this paper, we utilize PQ in long context LLM inference to ensure both effectiveness and efficiency. For potential future extensions involving IVF or other ANNS techniques, please refer to Section 5 for further discussion.

## 2.3 GPU-CPU Memory Hierarchy

Modern deep learning tasks heavily rely on GPUs for executing compute-intensive operations. The GPU-CPU structure forms a typical memory hierarchy: the more expensive GPU memory offers faster memory I/O speeds for computation, while the CPU memory, connected via PCI-e or NVLink, provides lower bandwidth. This memory hierarchy and the GPU-CPU interconnect is common

in modern GPU-equipped servers utilized in cloud environments [95, 97], data centers [40, 105], and edge devices [56, 92]. This hardware setting allows us to leverage available CPU memory for better efficiency when GPU memory is insufficient. As model parameters increase and the demand for intermediate results storage (such as KVCache) grows, CPUs are often employed to share the memory load. Numerous research studies in machine learning systems propose offloading certain model parameters or activations to the CPU memory [9, 36, 68, 74, 75, 78, 81, 99], thereby enhancing the overall performance of GPU-centric deep learning tasks. Similar to these studies addressing memory bottlenecks in deep learning models, we also treat GPU memory as a premium, high-bandwidth resource and consider CPU memory a secondary tier. The primary challenge in this context is to effectively schedule memory I/O (or say GPU-CPU communication) in conjunction with GPU computation to efficiently hide the associated overhead. It is worth noting that, although we currently implement PQCache within the GPU-CPU memory hierarchy, it can also be extended to incorporate disk storage – thereby adding another level to the memory hierarchy – to accommodate environments with limited resources in the future.

### 3 PQCache

In this section, we introduce PQCache, a novel system-algorithm co-designed method to enable effective and efficient long context LLM inference with large-scale KVCache. Figure 5 provides an overview of PQCache, where the KVCache from the prefilling phase is first offloaded to CPU, compressed using PQ, then fetched on demand during the decoding phase.

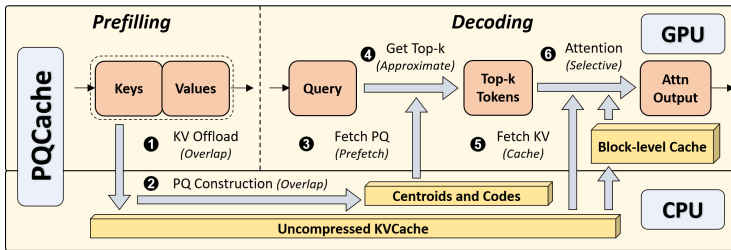


Fig. 5. An overview of PQCache. For simplicity, we only illustrate the process for a single transformer layer.

#### 3.1 Overview

We design PQCache to reserve all the KVCache in CPU, and selectively fetch relevant key-value pairs for self-attention computation. In long context inference scenario, the entire KVCache is too large for both attention computation and I/O communication within the memory hierarchy. Therefore, a common technique is to only perform attention on a subset of the key-value pairs, a process known as “selective attention”. According to previous research [2, 33, 59, 77, 79, 93, 99, 102, 112], attention score is a proper metric to measure the importance or relevance of previous tokens. As shown in Figure 6, we plot the attention score distributions at several randomly-selected positions on an example from a common summarization dataset XSUM [66]. The attention scores generally follow powerlaw distributions, indicating that a small part of tokens are more important than most other tokens. Therefore, we can only include those tokens with large scores for self-attention computation. Following prior works [37, 100, 112], we also include initial tokens and the most recent tokens (called local tokens) in attention computation.

As detailed in Section 2.1, attention scores are calculated using a softmax function applied to the product of the current query and preceding keys. The procedure of identifying the top- $k$  keys with

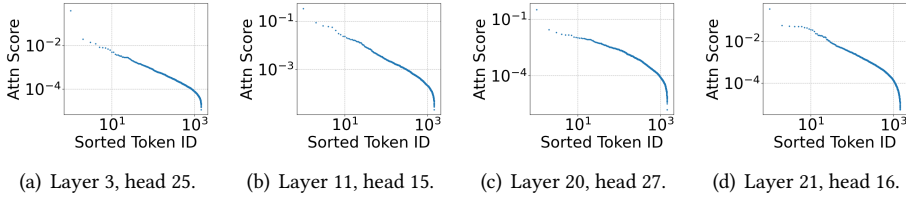


Fig. 6. Distributions of attention scores.

the highest scores fundamentally constitutes an Approximate Nearest Neighbor Search (ANNS) operation. Therefore, we try to leverage embedding retrieval techniques to enable effective selective attention and address the KVCache memory issue. Based on the observations above, we design PQCache, which offloads all the KVCache to CPU, and fetch only relevant tokens' key-values pairs during the decoding phase. Calculating exact attention scores of all previous tokens involves costly I/O communication, which is unacceptable in long context LLM inference. Inspired by ANNS in information retrieval [11, 43, 48], we leverage the light-weight Product Quantization (PQ) method [44], which compress the vectors by partitioning and K-Means clustering. Though there are other ANNS methods (e.g. graph-based methods [28, 43, 62]) that can achieve better recall performance, they suffer from a computationally expensive construction process which may hinder LLM inference.

In PQCache, we construct PQ during the prefilling phase and utilize PQ during the decoding phase. We use tensors to manage all PQ-related data structures, which are natively supported by deep learning frameworks including PyTorch [71], TensorFlow [1], and Hetu [63]. The following is a detailed explanation of how PQCache operates, as illustrated in Figure 5.

**Step ①:** During the prefilling phase, we calculate all the input tokens' keys and values at each layer. Both the keys and values have the shape of  $(n, h_{kv}, s, d_h)$ . They are then asynchronously offloaded to CPU, a process that can overlap with subsequent computations.

**Step ②:** We perform PQ construction on CPU. We omit the batch size and head dimensions for simplicity, and get per-head key vector of shape  $(s, d_h)$ . We then divide the dimension  $d_h$  into  $m$  sub-spaces with dimension  $d_m$ . For partitioned vectors  $(m, s, d_m)$ , where  $d_m = d_h/m$ , we conduct K-Means clustering for each group separately, resulting in centroids of shape  $(m, 2^b, d_m)$  and PQ codes of shape  $(s, m)$ . Each PQ code, which indicates the cluster to which the vector belongs, requires only  $b$  bits for storage.

**Step ③:** During the decoding phase, while computing the previous transformer layer, we pre-fetch PQ centroids and codes. While the PQ codes are linear with sequence length, the centroids are of small volume and can be kept on GPU throughout the inference.

**Step ④:** We perform PQ search on GPU: first conducting matrix multiplication between the query and the PQ centroids, then aggregating the result with PQ codes to obtain the approximate scores for all tokens. We can then identify the top- $k$  relevant tokens using the approximate scores.

**Step ⑤:** Using the PQ scores, we fetch the approximate top- $k$  tokens' key-value pairs from CPU, or from a GPU cache which we will discuss later in Section 3.4.

**Step ⑥:** The selective self-attention computation continues with the retrieved tokens.

Unlike typical embedding retrieval tasks, in LLM inference, newly generated keys and values are added to the KVCache. These tokens are initially considered as local tokens and reserved in GPU. When they are evicted from the sliding window of local tokens, they are assigned PQ codes based on their nearest centroids.

### 3.2 Complexity Analysis

In this section, we analyze the time and space complexity in PQCache-equipped LLM inference. During prefilling, the attention computation remains unmodified, thus the time and memory complexity stay the same. Concretely, the matrix multiplications in attention and FFN have the tensor shapes of  $(h, s, d_h) \times (h, d_h, s) \rightarrow (h, s, s)$ ,  $(h, s, s) \times (h, s, d_h) \rightarrow (h, s, d_h)$ , and  $(s, d) \times (d, d) \rightarrow (s, d)$ , yielding a time complexity of  $O(s^2d/h + sd^2)$ . In current long-context training and inference of LLMs, FlashAttention [21, 22] has become the de facto implementation of attention computation. It implements tiled multiplication and softmax, resulting in a space complexity of  $O(sd)$ . While the details of FlashAttention are not the focus of our paper, it's worth noting that in our experiments, FlashAttention is utilized by baselines and PQCache by default, except for H2O due to compatibility issues. Using PQCache, the additional K-Means clustering process has an average complexity of  $O(sh_{k_v}md_m2^bT)$ , where  $T$  is the number of K-Means iterations. Its complexity is linear with the input sequence length. We leverage idle CPU resources to perform K-Means, allowing the clustering to overlap with GPU computation, which will be detailed in Section 3.3.

During the decoding phase, the matrix multiplications in the original LLM have the tensor shapes of  $(h, 1, d_h) \times (h, d_h, s) \rightarrow (h, 1, s)$ ,  $(h, 1, s) \times (h, s, d_h) \rightarrow (h, 1, d_h)$ , and  $(1, d) \times (d, d) \rightarrow (1, d)$ , leading to a time complexity of  $O(sd + d^2)$ . Using PQCache, we first multiply the query with PQ centroids, which has shapes of  $(h, m, 1, d_m) \times (h, m, d_m, 2^b) \rightarrow (h, m, 1, 2^b)$ , then gather and reduce using PQ codes, which has shapes of  $(h_{k_v}, s, m)(h_{k_v}, m, 1) \rightarrow (h_{k_v}, s)$ . The PQ-related process has a time complexity of  $O(2^b d^2 / (hm) + h_{k_v}ms)$ . Finding the top- $k$  largest scores has a time complexity of  $O(h_{k_v}s)$ , since PyTorch tends to use a radix-sort-like algorithm to determine the  $k$ -th large element. Computing the selective attention and the subsequent FFN has a time complexity of  $O(kd + d^2)$ . Therefore, the overall time complexity is  $O(2^b d^2 / (hm) + h_{k_v}ms + kd + d^2)$ . The memory complexity of PQ centroids and codes is  $O(h_{k_v}ms + h_{k_v}2^b \cdot d_h)$ . In long-context scenarios, we focus on the multipliers of  $s$ . For time complexity, current multiplier  $h_{k_v}m$  is much smaller than the original  $d$ , considering  $h_{k_v}m \ll d$  (e.g.  $h_{k_v}=8, m=2, d=4096$  in 7B model). For space complexity, the small size of  $h_{k_v}m$  allows the communication of PQ structures to overlap with GPU computation. Consequently, PQCache enables more efficient decoding.

To facilitate efficient long context LLM inference, the design goal of PQCache is to provide overhead-agnostic service. Figure 7 illustrates the computation and communication involved in the PQCache-enabled LLM inference, covering both the prefilling and decoding phases. The original LLM computation is filled with blue color, while the computation and the communication introduced by PQCache are filled with green and red colors, which can be divided into four parts: (1) KVCache offloading and PQ structure fetching; (2) PQ construction using K-Means clustering; (3) Approximate top- $k$  computation; (4) The fetch process of top- $k$  relevant tokens' key-value pairs. As shown in Figure 7, except for the low-cost top- $k$  approximation, we employ distinct system design to eliminate these computation or communication overhead. The system design is detailed in the following sections.

### 3.3 Prefilling Phase

During the prefilling phase, GPU computations, GPU-to-CPU offload communications, and PQ construction can all be executed concurrently. The process is depicted in Figure 7(a) and Algorithm 1. Lines 3-8 illustrate the GPU computations. Within each layer, the input is initially projected into queries, keys, and values, respectively. The keys and values are then asynchronously transferred to the CPU. Meanwhile, the GPU continues with computations for the attention and feed-forward network operations. Following the transformer layers, the classifier layer performs matrix multiplication and applies a softmax function to predict the next token. Lines 9-13 and lines 14-17

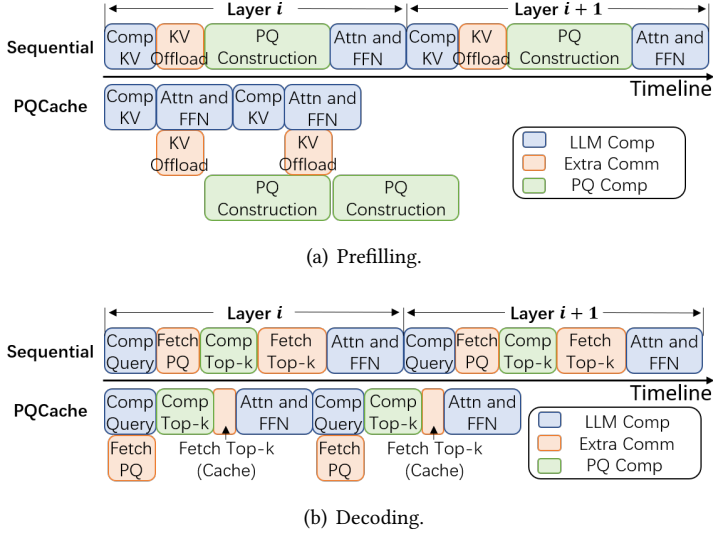


Fig. 7. PQCache v.s. sequential scheduling.

**Algorithm 1:** PQCache prefilling phase

---

**Input** : Tokenized query  $X$   
**Output** : Output token; KVCache; PQ structures

```

1 ProcComm = ProcPQ = KVCache = PQ = {};
2  $L_x = X.length()$ ;
  // Prefilling computation on GPU
3 for  $i \leftarrow 0$  to  $L - 1$  do
4    $Q, K, V = Projection_i(X)$ ;
5   ProcComm.append(AsyncGPU2CPU( $K, V$ ));
6    $X = AttnFFN_i(Q, K, V)$ ;
7 end
8 Token = Classifier( $X$ );
  // Launch PQ construction on CPU
9 for  $i \leftarrow 0$  to  $L - 1$  do
10   $K, V = ProcComm[i].sync()$ ;
11  KVCache.append( $(K, V)$ );
12  ProcPQ.append(AsyncPQConstruct( $K, L_x$ ));
13 end
  // Wait for PQ construction in the next decoding phase
14 for  $i \leftarrow 0$  to  $L - 1$  do
15  Centroids, Codes = ProcPQ[ $i$ ].sync();
16  PQ.append( $(Centroids, Codes)$ );
  // Some decoding logic here
17 end
18 return Token, KVCache, PQ

```

---

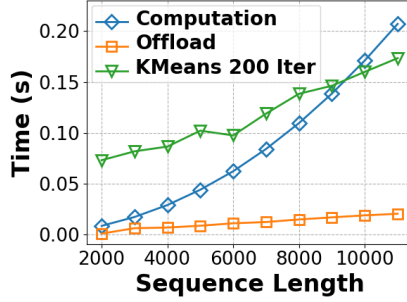


Fig. 8. The execution time of one-layer transformer computation, offloading, and clustering at the prefiling phase.

demonstrate the initiation and waiting period of PQ construction, respectively. Upon acquiring the keys and values, a separate process on CPU launches multiple clustering processes for PQ construction. Given the distinct latent spaces of different heads in transformers  $h_{kv}$  and different groups in PQ  $m$ , these clustering processes, totaling  $h_{kv}m$  per layer per sample, can operate in parallel. To enable on-demand synchronization, we wait for PQ construction to complete at the same transformer layer of the next token decoding phase.

Figure 8 shows the time usage of a 7B LLM single-layer transformer computation on an NVIDIA RTX 4090 GPU, GPU-to-CPU communication via PCI-e 1.0 (x16), and PQ construction (K-Means clustering processes) on two Intel(R) Xeon(R) Gold 6330 CPUs, with the input sequence lengths varying. Given that the attention computation time scales quadratically with sequence length, while both the communication time and the K-Means clustering time scale linearly, the computation can entirely encompass the other two operations when the sequence length is sufficiently long. In such cases, we can fully utilize the idle CPU and PCI-e resources. However, when the sequence length is insufficient, the duration of the K-Means clustering may exceed that of the GPU computation. This issue may become increasingly pronounced as GPU computation capability advances over the years.

To address this issue and ensure that the clustering can be overlapped by GPU computation, we propose an adaptive K-Means method that limits the maximum number of iterations for clustering. Given the complexity of K-Means as discussed in Section 3.2, we fit a linear curve of K-Means clustering time as follows:

$$Time_{clus} = \alpha_1 + \beta_1 \cdot sT. \quad (1)$$

Here  $s$  is the sequence length, and  $T$  is the number of iterations. Meanwhile, the GPU computation time can be fitted as a quadratical relation:

$$Time_{comp} = \alpha_2 + \beta_2 \cdot s + \gamma_2 \cdot s^2, \quad (2)$$

The maximum number of iterations, denoted as  $T_{max}$ , that ensures clustering does not interfere computation should satisfy  $Time_{clus} = Time_{comp}$ , which yields:

$$T_{max} = \frac{\gamma_2 \cdot s^2 + \beta_2 \cdot s + \alpha_2 - \alpha_1}{\beta_1 \cdot s}. \quad (3)$$

In practice, we also clip  $T_{max}$  to ensure that the number of iterations is neither too small nor too large. For any given models and devices, we can profile time of single-layer computation and clustering time using several input sequence lengths, then employ a simple regression technique to fit the coefficients  $\alpha_1, \beta_1, \alpha_2, \beta_2, \gamma_2$ . By modeling the relationship between computation time and sequence

length, we can determine the maximum number of K-Means iterations as Eq 3. In Section 4.3.4, we empirically study the trade-off between the efficiency and model quality of different clustering iterations.

---

**Algorithm 2:** PQCache decoding phase
 

---

```

Input : Last generated token  $X$ 
State : InitKV; MidKV; LocalKV; PQ codes; PQ centroids
Output: Output token
// First pre-fetch first layer's PQ codes
1  $Proc = AsyncCPU2GPU(PQCodes[0]);$ 
2 for  $i \leftarrow 0$  to  $L - 1$  do
    // Evict previous token from local tokens
3    $EvictK, EvictV = LocalKV.pop(0);$ 
4    $NewCode = PQArgNearest(EvictK);$ 
    // On CPU, MidKV and PQ will be updated
5    $AsyncGPU2CPU((NewCode, EvictK, EvictV));$ 
    // Get Q, K, V for last token
6    $Q, K, V = Proj_i(X);$ 
    // Get KV for current attention
7    $LocalKV.append((K, V));$ 
8    $Codes = Proc.sync();$ 
9    $Centroids = PQCentroids[i];$ 
10  if  $i \neq L - 1$  then
    // Pre-fetch next layer's PQ codes
11  |  $Proc = AsyncCPU2GPU(PQCodes[i + 1]);$ 
12  end
13   $Codes.append(NewCode);$ 
14   $TopkToken = PQSearch(X, Centroids, Codes);$ 
15   $TopkKV = SyncFetchKV(TopkToken);$ 
16   $AllKV = InitKV + TopkKV + LocalKV;$ 
    // Continue attention and FFN computation
17   $X = AttnFFN_i(Q, AllKV);$ 
18 end
19  $Token = Classifier(X);$ 
20 return Token
  
```

---

### 3.4 Decoding Phase

Algorithm 2 outlines the decoding phase of PQCache. During this phase, the constructed PQ structure is utilized by the attention module in each layer. The PQ centroids are directly stored on GPU, since they consume a fixed and negligible amount of memory (e.g., only 16M for  $m = 2, b = 6, 7B$  GQA LLM), and are independent of sequence length. As the preceding layer's computation progresses, the PQ codes for the next layer can be pre-fetched in parallel, as indicated in line 1 and lines 9-11. Given the significantly smaller size of the PQ codes compared to original keys, their communication can overlap with the decoding phase computation.

We partition the entire KVCache into three segments: initial tokens, middle tokens, and local tokens. The key-value pairs of initial and local tokens (the most recently generated tokens) are directly involved in attention computation and are therefore stored on GPU. Conversely, the key-value pairs of middle tokens are stored on CPU. In each transformer layer, local tokens first evict the earliest token, generate its PQ codes, and asynchronously offload its key and value to the CPU, as depicted in lines 3-5. The newly generated key and value are then added to the local tokens, as shown in lines 6-7. Upon receiving the PQ codes from the CPU in line 8, a PQ search is conducted to identify the top- $k$  tokens in lines 12-13. After fetching these tokens' keys and values from CPU in line 14, we obtain all keys and values for attention in line 15, and the computation continues in line 16.

The only communication that cannot be overlapped is the retrieval of the top- $k$  relevant tokens, as it relies on the preceding PQ search. Inspired by previous research [59, 99, 112], there are certain pivotal tokens that are consistently important during inference. To accommodate these tokens, we design a block-level GPU cache, employing either a Least Frequently Used (LFU) or Least Recently Used (LRU) eviction policy. On identifying the top- $k$  tokens, we first check the cache for their availability. For tokens already in the cache, we directly retrieve their keys and values. For those not in the cache, we fetch them from CPU. After retrieving keys and values, we asynchronously update the cache, adding and evicting tokens according to the eviction policy. This update process, only involves PCI-e communication, does not interfere with GPU computation. To minimize cache-lookup overhead, we leverage block-level granularity over token-level granularity. We partition all tokens into blocks and store frequently-used blocks in the GPU cache. During each retrieval, we update the cache using the top- $k_{cache}$  blocks, which contain the most top- $k$  tokens. Here  $k_{cache}$  refers to the number of blocks, while  $k$  specifies the number of tokens. Experimental results in Section 4.3.2 demonstrate the effectiveness of the GPU cache in reducing latency.

## 4 Experiments

In this section, we conduct experiments and compare PQCache with existing methods. We experimentally show that PQCache achieves both effectiveness and efficiency.

### 4.1 Experimental Setup

**4.1.1 Models.** We conduct experiments using two representative open-source LLMs: Llama-3.1-8B [26] and Mistral-7B-Instruct-v0.2 [45], which support context lengths of 128K and 32K, respectively. Both models employ GQA and share similar architectures. Following common practice, we use FP16 for model inference.

**4.1.2 Tasks.** We evaluate PQCache on two multitask benchmarks for long context inference: LongBench [10] and InfiniteBench [111]. These benchmarks are widely evaluated in related research works [14, 33, 52, 79, 85, 93, 99]. The evaluation tasks encompass question answering, summarization, few-shot learning, multiple choice, and retrieval. Detailed meta information such as sample lengths, task descriptions, and metrics is available on LongBench<sup>1</sup> and InfiniteBench<sup>2</sup> websites. Tasks in LongBench typically average 10k in length, while those in InfiniteBench average 100k, which is significantly longer. Each task employs a specific evaluation metric, such as accuracy, Rouge-L, or F1-score, which we simply call "score". Consistent with previous work, we report the scores of the tasks and their average.

We also experiment on two additional tasks: the Needle-in-a-Haystack [49] and the GSM8k Chain-of-Thought (CoT) reasoning [94]. The Needle-in-a-Haystack test evaluates the in-context

<sup>1</sup><https://github.com/THUDM/LongBench/tree/main/LongBench>

<sup>2</sup><https://github.com/OpenBMB/InfiniteBench>

retrieval ability of long-context LLMs by asking the model to retrieve a random fact or statement placed from a lengthy document. This test is conducted on documents with various lengths to determine the model’s retrieval accuracy. In our experiments, we consider up to 128K document length. GSM8k is a math reasoning dataset containing 8k high quality diverse grade school math problems. Its CoT variant is a complex reasoning task that require model to attend to extensive contextual details for accurate answers, with an average input length of 3.7k. The accuracy metric measures if the model can correctly answer the questions.

**4.1.3 Baselines.** We compare with the following baselines:

- **H2O** [112] uses accumulative attention scores to determine which key-values pairs to retain.
- **SnapKV** [52] analyzes the attention scores from the prompt’s last segment to identify important tokens and employs pooling to preserve their surrounding information.
- **PyramidKV** [14] improves over SnapKV by allocating more budget to lower layers and less to higher layers.
- **SPARQ** [79] selects dimensions with the largest magnitudes in query tensors, and retrieves these dimensions from all tokens’ keys to determine the top- $k$  tokens for attention.
- **InfLLM** [99] organizes tensors into blocks and uses representative tokens to identify important blocks for attention.

Among the baselines, H2O, SnapKV, and PyramidKV are KVCache dropping methods, while SPARQ and InfLLM are KVCache offloading methods. In addition, we consider an “Oracle” method that retrieves the exact top- $k$  tokens for each head. In our experiments, we align the number of tokens for selective attention and the data transfer amount in Oracle, SPARQ, InfLLM, and PQCache, to achieve a fair comparison. In experiments on model quality, we allow KVCache dropping methods (H2O, SnapKV, PyramidKV) to attend to more tokens, matching the memory usage of the selected key-value pairs and the data transfer amount in the other methods, following the experiment settings in SPARQ. We add a suffix of (C) to these methods, where “C” means compensation.

In our experiments, we specify two hyperparameters. The first is the ratio of previous tokens that participate in selective attention. For example, if the ratio is set to  $1/5$ , we only use  $s/5$  tokens for attention computation from an input sequence length of  $s$ . The second hyper-parameter is the ratio of extra communication relative to the original tokens’ keys, which we set to  $1/128$  in LongBench and  $1/64$  in InfiniteBench. For PQCache, we set  $m = 2, b = 6$  in LongBench, and set  $m = 4, b = 8$  in InfiniteBench. In each layer, we need to fetch PQ codes, which occupy  $h_{kv}msb/8$  bytes, as each code only requires  $b$  bits. The original tokens’ keys, using FP16, consume  $2h_{kv}sd_h$  bytes. In LongBench, since  $(h_{kv}msb/8)/(2h_{kv}sd_h) = mb/(16d_h) = b/8 \times 1/128 \leq 1/128$ , PQCache satisfies the  $1/128$  ratio requirement. In InfiniteBench, the calculation yields  $mb/(16d_h) = 1/64$ . For SPARQ, which retrieves  $r$  values from  $d_h = 128$  values, we set  $r = 1$  for  $1/128$  and  $r = 2$  for  $1/64$ . For InfLLM, we use 1 or 2 representative token from every 128 tokens.

**4.1.4 Hardware Environment and Hyperparameters.** Unless otherwise specified, for each experiment, we use an NVIDIA GeForce RTX 4090 24GB card for GPU computation, two Intel(R) Xeon(R) Gold 6330 CPUs for K-Means clustering, 500GB CPU memory, and PCI-e 1.0 (x16) for communication. For PQ construction in each layer, we have  $m * h_{kv}$  clustering processes, each executed using 4 CPU threads. For the GPU cache, we use 128 tokens per block to reduce management overhead. For other hyperparameters, we align them with the settings from the corresponding papers or open-source codes. It’s important to note that in our experimental figures, “k” represents 1000, while “K” represents 1024. In model performance experiments that require more memory than a single GPU card can provide, such as H2O (incompatible with FlashAttention), we utilize two or more GPU cards to partition the model.

## 4.2 Model Performance

**4.2.1 LongBench Evaluation.** The LongBench evaluation results on Llama-3.1-8B are presented in Table 2. We experiment using 1/5 and 1/10 of the input tokens in selective attention, with an extra communication equivalent to 1/128 of the memory used by the previous tokens’ keys. Excluding Oracle, the best results for each setting, are highlighted in bold. We also experiment on the Mistral-7B-inst-v0.2 model, with results presented in Appendix A.

Table 2. LongBench evaluation of the Llama-3.1-8B model (128K context length). “Ora” stands for Oracle. “H(C)”, “S(C)”, and “P(C)” represent H2O, SnapKV, and PyramidKV, which are configured with extra tokens such that the memory usage matches that of other methods’ selected tokens and transferred data amount. “Inf”, “SPA”, and “PQC” denote InfLLM, SPARQ and PQCache, which all involve extra communications at an amount of 1/128 keys memory for pre-calculating relevance.

Dataset	Full	1/5 #Tokens + 1/128 Extra Comm							1/10 #Tokens + 1/128 Extra Comm						
		Ora	H(C)	S(C)	P(C)	Inf	SPA	PQC	Ora	H(C)	S(C)	P(C)	Inf	SPA	PQC
NarrativeQA	29.91	30.30	<b>30.94</b>	30.02	30.50	26.00	28.82	30.08	30.92	29.02	30.36	<b>31.12</b>	21.06	29.24	30.14
Qasper	44.79	44.57	37.38	42.55	43.65	35.07	35.11	<b>44.93</b>	44.82	34.08	39.05	39.09	23.93	30.28	<b>44.36</b>
MultiFieldQA	54.63	54.68	48.80	54.43	54.30	42.92	48.34	<b>55.11</b>	54.62	45.66	53.71	53.07	37.90	43.38	<b>54.97</b>
HotpotQA	55.81	55.98	55.50	<b>56.59</b>	55.75	46.42	53.86	55.60	55.98	54.39	56.05	55.89	41.96	52.52	<b>56.35</b>
2WikiMQA	45.78	46.16	45.23	46.02	<b>46.32</b>	27.81	45.24	45.89	46.59	44.23	45.04	45.61	23.66	45.40	<b>45.79</b>
Musique	30.41	30.36	28.38	30.32	30.44	21.60	28.27	<b>30.50</b>	30.68	27.19	<b>30.29</b>	29.92	18.14	26.72	30.15
GovReport	35.23	35.01	32.41	30.06	29.77	32.42	29.37	<b>34.29</b>	34.78	30.25	27.15	26.81	30.89	26.87	<b>33.97</b>
QMSum	25.11	25.52	24.53	24.77	24.91	23.55	23.82	<b>25.67</b>	25.23	23.60	24.74	24.90	21.80	23.60	<b>25.24</b>
MultiNews	27.30	26.70	26.28	24.26	23.40	24.98	24.42	<b>26.33</b>	26.78	25.30	22.65	22.08	23.48	22.78	<b>25.95</b>
TREC	72.50	72.50	69.00	70.00	70.50	61.50	64.50	<b>72.50</b>	72.50	67.50	66.50	66.50	53.00	54.00	<b>72.00</b>
TriviaQA	91.65	91.48	91.88	92.17	<b>92.30</b>	87.53	91.15	91.79	91.76	91.34	91.72	<b>92.34</b>	83.41	90.69	91.65
SAMSum	43.80	43.57	42.68	42.89	42.71	42.99	43.27	<b>43.66</b>	43.95	42.73	42.38	41.94	42.77	42.76	<b>43.34</b>
Count	6.72	7.22	<b>6.81</b>	6.72	6.72	3.00	6.22	6.72	7.22	<b>6.72</b>	6.72	6.72	4.00	6.23	<b>6.72</b>
Retrieval	99.50	99.50	94.50	<b>99.50</b>	<b>99.50</b>	83.50	97.00	99.00	99.50	90.50	<b>99.50</b>	<b>99.50</b>	55.00	96.50	<b>100</b>
Average	47.37	47.40	45.31	46.45	46.48	39.95	44.24	<b>47.29</b>	47.52	43.75	45.42	45.39	34.36	42.21	<b>47.19</b>

Compared to the baselines, PQCache achieves an improvement of +1.74% using 1/5 #tokens and +3.90% using 1/10 #tokens. The offloading-based baseline methods, InfLLM and SPARQ, do not perform well, as we limit additional communication to minimize latency. SnapKV(C) and PyramidKV(C), which assume that the last segment of the input context provides crucial token importance information, perform well in the benchmarks and tasks in this paper, particularly because the input questions are consistently positioned at the end of the context. In later paragraphs, we conduct further experiments demonstrating that SnapKV(C) and PyramidKV(C) fail to match the performance of PQCache when questions are not positioned at the end. Despite KVCache dropping baselines using more tokens for compensation and making specific assumptions on question positioning, PQCache outperforms all these methods, demonstrating superior generation performance. On most datasets, PQCache performs the best. While a small number of tasks see some baseline methods slightly outperforming PQCache, the differences are not substantial.

The column “Full” shows model performance without compression. However, it seems “Oracle”, which uses ideally top- $k$  selective attention, performs even better. There are mainly two reasons. (1) In LongBench, when the sequence length exceeds the model’s maximum context length, only the initial and the last tokens are used [10]. (2) Selective attention only focuses on the tokens that really matters, which makes the generation perform better. Compared to “Oracle”, PQCache achieves comparable results, with an average difference of less than 0.70%. This difference is 6.36 times smaller than that of other baselines. In some cases, we observe that PQCache even beats “Oracle”. This suggests that clustering may help PQCache uncover intrinsic structures within the KVCache latent space, thus leading to promising results. Furthermore, although it is usually expected that

the performance should drop when there are fewer tokens, there are exceptions where the opposite happens. This could be because not all tokens are useful for generating new ones, so getting rid of unnecessary ones might enhance inference.

Table 3. LongBench question-answering tasks evaluation using Llama-3.1-8B, with questions placed before other contexts. (1/10 #Tokens, 1/128 extra communication)

Dataset	S(C)	P(C)	PQC
NarrativeQA	<b>19.39</b>	19.35	18.82
Qasper	18.70	17.60	<b>25.76</b>
MultiFieldQA	43.48	44.07	<b>47.99</b>
HotpotQA	42.93	42.55	<b>43.28</b>
2WikiMQA	36.36	35.04	<b>36.48</b>
Musique	20.86	21.19	<b>22.29</b>
Average	30.29	29.97	<b>32.44</b>

Since the strong baselines SnapKV(C) and PyramidKV(C) rely on the assumption that the last segment of the input, typically the question, can determine the important tokens, we experiment on an alternative setup where the questions are not placed at the end. Specifically, we position the questions before the other contexts in the question-answering tasks of LongBench. As shown in Table 3, as we alter the positions of the input elements without further tuning the prompt, the overall results are inferior to those from the standard LongBench evaluation. In this modified scenario, PQCache demonstrates superior performance over SnapKV(C) and PyramidKV(C) across nearly all datasets, achieving a significant improvement of +7.10%. Though SnapKV(C) and PyramidKV(C) perform well in the benchmarks and tasks evaluated in this paper where questions are typically positioned at the end of the input, their performance declines in scenarios with varied question placements – situations that frequently occur in real-world applications. In contrast, PQCache, which does not rely on assumptions beyond selective attention, offers greater robustness and adaptability across various scenarios.

Table 4. Infinitebench evaluation of the Llama-3.1-8B model (128K context length). “Ora” stands for Oracle. “H(C)”, “S(C)”, and “P(C)” represent H2O, SnapKV, and PyramidKV, which are configured with extra tokens such that the memory usage matches that of other methods’ selected tokens and transferred data amount. “Inf”, “SPA”, and “PQC” denote InLLM, SPARQ and PQCache, which all involve extra communications at an amount of 1/64 keys memory for pre-calculating relevance.

Dataset	Full	1/5 #Tokens + 1/64 Extra Comm						1/10 #Tokens + 1/64 Extra Comm							
		Ora	H(C)	S(C)	P(C)	Inf	SPA	PQC	Ora	H(C)	S(C)	P(C)	Inf	SPA	PQC
En.Sum	27.41	26.91	26.97	26.05	26.22	22.49	26.20	<b>27.66</b>	26.88	26.55	26.04	26.03	24.85	25.36	<b>26.84</b>
En.QA	15.12	15.06	15.13	15.26	15.08	8.28	14.72	<b>15.45</b>	15.07	14.49	15.07	15.24	15.22	<b>15.34</b>	15.17
En.MC	67.25	67.25	<b>67.25</b>	<b>67.25</b>	<b>67.25</b>	54.59	<b>67.25</b>	<b>67.25</b>	67.25	67.25	67.25	67.25	51.97	<b>67.69</b>	67.25
En.Dia	16.50	16.50	<b>21.00</b>	16.50	14.00	9.00	15.50	17.00	18.50	19.00	16.50	13.00	12.00	15.50	<b>21.50</b>
Zh.QA	13.05	13.10	13.04	<b>13.49</b>	12.94	10.56	13.08	13.05	13.28	12.56	13.31	13.15	11.29	12.48	<b>13.41</b>
Math.Find	34.29	33.71	33.71	<b>34.29</b>	<b>34.29</b>	26.00	<b>34.29</b>	34.00	33.71	34.00	<b>34.29</b>	<b>34.29</b>	34.00	<b>34.29</b>	34.00
Retr.PassKey	100	100	<b>100</b>	<b>100</b>	<b>100</b>	65.59	<b>100</b>	<b>100</b>	100	99.32	<b>100</b>	<b>100</b>	<b>100</b>	<b>100</b>	<b>100</b>
Retr.Number	99.49	99.32	90.68	<b>99.49</b>	<b>99.49</b>	54.41	87.46	96.78	98.31	77.97	99.32	99.49	<b>100</b>	83.39	93.39
Retr.KV	55.60	56.20	8.40	44.60	50.20	2.60	8.00	<b>54.60</b>	55.40	4.60	30.60	34.20	3.40	4.00	<b>49.60</b>
Average	47.63	47.56	41.80	46.33	46.61	28.17	40.72	<b>47.31</b>	47.60	39.53	44.71	44.74	39.19	39.78	<b>46.80</b>

**4.2.2 InfiniteBench Evaluation.** The InfiniteBench results on Llama-3.1-8B are presented in Table 4. The experiment uses 1/5 and 1/10 of the input tokens in selective attention, with an extra communication equivalent to 1/64 of the memory used by the tokens’ keys. We use increased

communication in InfiniteBench due to its much longer input contexts (around 100k). Excluding Oracle, the best results for each setting, are highlighted in bold.

Compared to the baselines, PQCache performs the best and achieves an improvement of +1.50% using 1/5 #tokens and +4.60% using 1/10 #tokens. Though SnapKV(C) and PyramidKV(C) perform well because questions are typically positioned at the end of the input context, PQCache still achieves superior performance. On most datasets, PQCache performs the best and exhibits negligible degradation compared to Full and Oracle. Although some baselines may perform better in specific tasks, PQCache consistently achieves scores that are very close. PQCache achieves results comparable to Oracle, with an average difference of less than 1.71%. This difference is 3.58 times smaller than that of other baselines.

**4.2.3 Large-scale Needle-in-a-Haystack.** We use the Llama-3.1-8B model to conduct the needle-in-a-haystack test. We employ the common setting [6]: the “haystack” is Paul Graham’s Essays, and the “needle” is “*The best thing to do in San Francisco is eat a sandwich and sit in Dolores Park on a sunny day.*” For each experiment, we use 1/10 the number of tokens in selective attention, and 1/64 extra communication. We use increased communication due to the long input contexts. The results are shown in Figure 9, where the x-axis represents the “haystack” length and the y-axis represents the position that the “needle” hides. We significantly extend the maximum length to a large scale, specifically 131,000 tokens, as Llama-3.1-8B supports a maximum context length of  $128 \times 1024 = 131,072$  tokens. Greener shades indicate greater accuracy within the length range, demonstrating the model’s ability to effectively retrieve the “needle” from the “haystack”.

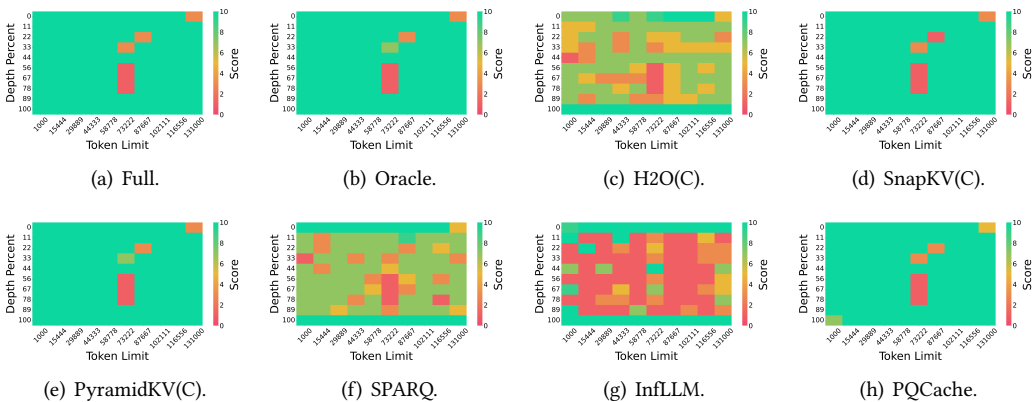


Fig. 9. Experimental results of the Needle-in-a-Haystack test.

Among all the methods, SnapKV(C), PyramidKV(C), and PQCache demonstrate superior performance, successfully locating the needle in most of the scenarios. These methods achieve performance nearly equivalent to Full and Oracle settings. SnapKV(C) and PyramidKV(C) involve more tokens and take advantage of the evaluation setting where questions appear in the final segment of the input context. PQCache, which involves minimal communication overhead and does not assume a specific position for the question, has shown promising results in large-scale scenarios. Other baseline methods, however, fail to retrieve the needle in a substantial amount of cases. InfLLM, in particular, struggles to find the needle in most cases, possibly due to its reliance on block-partitioning and the needle not being considered as representative tokens.

**4.2.4 Integrating with Prefilling Acceleration Method.** Given that PQCache primarily enhances the decoding phase, we attempt to integrate it with MInference [46], a state-of-the-art prefilling acceleration method. MInference designs sparse attention patterns during the prefilling phase to accelerate computation. As we experiment the default settings of MInference, the results, as shown in Table 5, indicate that MInference significantly degrades performance compared to dense attention baselines Full and PQCache. After combining MInference and PQCache, we can simultaneously accelerate prefilling phase and address the KVCache memory issue in decoding phase. Although faster prefilling shortens the clustering iterations of PQCache and sparse attention impacts the subsequent decoding process, PQCache still performs robustly. It exhibits only slight performance degradation compared to using MInference alone, demonstrating its strong compatibility with advanced prefilling acceleration methods.

Table 5. Performance of PQCache (1/5 #tokens, 1/64 communication) combined with MInference on InfiniteBench using Llama-3.1-8B. “PQC” stands for PQCache, “MInf” stands for MInference, and “Comb” stands for their combination.

Dataset	Full	PQC	MInf	Comb
En.Sum	27.41	27.66	26.58	25.22
En.QA	15.12	15.45	13.58	13.26
En.MC	67.25	67.25	58.95	58.95
En.Dia	16.50	17.00	12.50	11.50
Zh.QA	13.05	13.05	11.85	11.93
Math.Find	34.29	34.00	34.00	34.00
Retr.PassKey	100	100	100	100
Retr.Number	99.49	96.78	98.31	93.39
Retr.KV	55.60	54.60	13.60	13.40
Average	47.63	47.31	41.04	40.18

**4.2.5 Results on Larger Model.** To evaluate the performance of PQCache on larger LLMs, we conduct additional experiments using the Llama-3.1-70B model, with the results presented in Table 6. We employ pipeline parallelism [35, 42] to partition the model layers on four 80G A800 GPUs. We use 1/5 the number of tokens in selective attention and 1/128 extra communications. For CPU resources, we simulate two settings: in one, we use the same amount of CPU resources per GPU as in the 8B model experiment; in the other, we use half the amount. Still, the CPU computation employs limited clustering iterations to prevent GPU idle times and ensure efficiency. Compared to the 8B model in Section 4.2.1, Llama-3.1-70B demonstrates superior performance, since it has much more parameters. The performance gap between the non-compressed baseline and PQCache is negligible on the 70B model. This can be attributed to two main factors: (1) Larger model is equipped with enhanced capabilities and also demonstrates increased robustness to selective attention. (2) When using a larger GQA model for PQCache, each layer experiences an increased computational burden on GPU, while the clustering task on CPU remains the same. This is because in Llama, different model sizes have the same number of key-value heads<sup>3</sup>, which leads to the same complexity as analyzed in Section 3.2. Therefore, by using the same amount of CPU resources per GPU and assuming that each GPU processes a layer simultaneously, PQCache is expected to have more clustering iterations and perform better with larger models. As shown in Table 6, even when we halve the CPU resources per GPU, PQCache already achieves performance comparable to the non-compressed baseline.

<sup>3</sup>Note that this phenomenon generally applies to Llama-like models, although it may not be the case for some others, such as Qwen-2.5 [73]. We can employ the same analytical methodology for other models, and in most instances, the increase in PQ clustering computation is smaller than that of LLM computation as the model scales.

Table 6. LongBench evaluation of Llama-3.1-70B (128K). We simulate half / same amount of CPU resources per GPU as in the experiments on 8B model.

Dataset	Full	PQCache		Dataset	Full	PQCache	
		Half	Same			Half	Same
NarrativeQA	35.07	35.02	35.02	MultiNews	26.95	26.77	27.16
Qasper	49.97	49.25	49.02	TREC	76.50	76.50	76.00
MultifieldQA	54.20	54.19	54.25	TriviaQA	94.04	94.04	94.04
HotpotQA	64.95	65.07	64.95	SAMSum	47.37	47.67	47.47
2WikiMQA	67.85	67.68	67.68	Count	20.00	20.00	20.00
Musique	46.78	47.63	47.74	Retrieval	97.50	97.50	97.50
GovReport	34.65	34.80	34.84	<b>Average</b>	<b>52.89</b>	<b>52.88</b>	<b>52.86</b>
QMSum	24.56	24.22	24.37				

**4.2.6 GSM8k CoT Reasoning.** We use the Mistral-7B-inst-v0.2 model for GSM8k CoT Reasoning. Our prompt strategy involves 8 questions with 9-step reasoning and 2 questions with 8-step reasoning per sample, a common setup for long context inference [29]. We use 1/128 extra communications. As shown in Figure 10(a), PQCache consistently outperforms H2O, SnapKV(C), PyramidKV(C), SPARQ, and InFLLM across different token counts, demonstrating strong reasoning capabilities. Some results even surpass the uncompressed counterpart, suggesting that using part of the tokens can lead to improvements. H2O(C) performs better than PQCache using 1/10 number of tokens, as it is allowed to access more tokens.

**4.2.7 Impact of PQ Configuration.** We use Mistral-7B-inst-v0.2 to evaluate the effect of PQ configurations, including the number of partitions  $m$  and the number of centroids  $2^b$ . Figure 10(b) shows the results on HotPotQA and Qasper datasets with 1/10 tokens in selective attention, where the legends indicate  $m \times b$ . The maximum number of clustering iterations is set as described in Section 3.3 for each configuration, so as not to disturb GPU computation. To ensure that expensive configurations do not benefit unfairly from the clipped maximum number of clustering iterations, we are experimenting with a more aggressive clipping strategy, which permits a very small number of clustering iterations. As analyzed in Section 4.1.3, the involved communication is  $mb/(16d_h)$ . Therefore, as long as  $mb \leq 16$ , we can ensure that the extra communication will not exceed a size of 1/128 of tokens keys. From the figure, we can see that PQCache is robust across various PQ configurations, with all configurations performing well except for the  $8 \times 2$  setting on Qasper dataset. The configuration  $2 \times 6$  ( $m = 2, b = 6$ ) yields the best performance. It offers a sufficient number of centroids for representation, and in experiments it also has an appropriate number of clustering iterations. Therefore, we choose it as the default configuration.

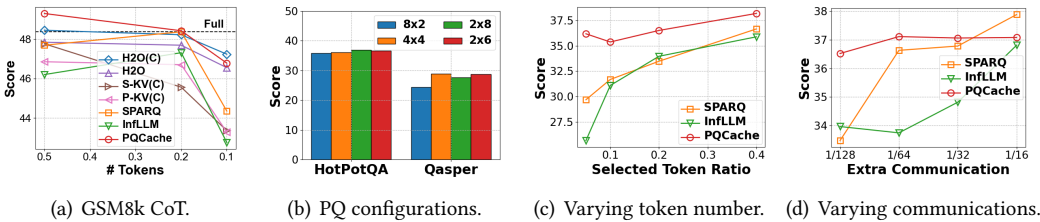


Fig. 10. (a) Performance on GSM8k with CoT. (b) Performance of PQCache with different PQ configurations. (c-d) Performance on HotPotQA under different settings.

**4.2.8 Variation in Token Number and Additional Communication.** We use Mistral-7B-inst-v0.2 to investigate how the number of involved tokens and the amount of extra communication impact model performance on the HotPotQA dataset. Fixing extra communication at 1/128 of the tokens' keys memory, we vary selected token ratio from 0.05 to 0.4. As shown in Figure 10(c), PQCache consistently outperforms the other baselines across different number of tokens. All methods exhibit an upward trend as the number of tokens increases. Fixing 1/5 of the tokens used, we vary the amount of extra communication from 1/128 to 1/16 of the tokens' keys memory. As shown in Figure 10(d), InfLLM and SPARQ has a upward trend when the communication increases, while PQCache remains stable. Using 1/128 communication, the PQ structure is sufficient for PQCache to achieve a promising score. In the 1/16 communication case, SPARQ achieves a slightly higher score than PQCache. However, SPARQ already incurs significant latency under the 1/128 case, as shown in Section 4.3.1. Even it performs well under the 1/16 case, the latency becomes increasingly unacceptable. In low-communication scenarios, which are suitable for practical usage, PQCache achieves the best model performance.

### 4.3 Efficiency

In LLM inference, both prefilling and decoding efficiency are crucial. When a user inputs a query, the LLM first performs prefilling to output the initial token, during which the user waits for a response. Therefore, lower prefilling latency is preferable. During the decoding phase, tokens are generated one by one, and the speed should match human reading speed.

**4.3.1 End-to-end Experiments.** In PQCache, K-Means clustering runs concurrently with GPU computation, affecting the generation of the second token rather than the first. Therefore, instead of evaluating Time To First Token (TTFT), we use Time To Second Token (TT2T) to assess system optimization. This metric accounts for both the query entry to LLM output time and KVCache management overhead. As shown in Figure 11(a), with overlapping and adaptive clustering, PQCache achieves nearly the lowest TT2T compared to baseline methods. H2O collects attention scores during prefilling, preventing the use of FlashAttention for acceleration and leading to OOM issues with lengthy input. SnapKV and PyramidKV introduce negligible overhead during prefilling, resulting in low latency comparable to PQCache. SPARQ, while having no prefilling overhead, suffers from a slow decoding process, resulting in higher TT2T. InfLLM incurs time overhead due to the setup required for block-level KVCache management.

Time Per Output Token (TPOT) measures the time of each decoding step. We present the TPOT of the methods in Figure 11(b). Here we use 1/5 number of tokens with 1/128 extra communication in selective attention, and a GPU cache capable of holding 4096 tokens' keys and values. To ensure a fair comparison, we allocate space in the GPU cache for our PQ centroids as well. SPARQ must complete the query computations to determine which dimension to fetch from CPU, making the communication dependent on these computations. The sequential processing leads to the highest latency among the methods, with the communication scaling linearly with the sequence length. Except for SPARQ, all the other methods exhibit per-token latency faster than the human reading speed, which is around 250 words ( $\approx 333$  tokens) per minute [115]. H2O, SnapKV, and PyramidKV avoid extra communications, while InfLLM and PQCache both leverage system optimizations to accelerate decoding. InfLLM's block-level token management allows it to efficiently gather data from the CPU; however, this block-level assumption negatively impacts the model's overall quality. PQCache incorporates prefetching and caching, achieving an acceptable TPOT while not degrading model quality. It also maintains a nearly stable TPOT that does not scale with increasing sequence length.

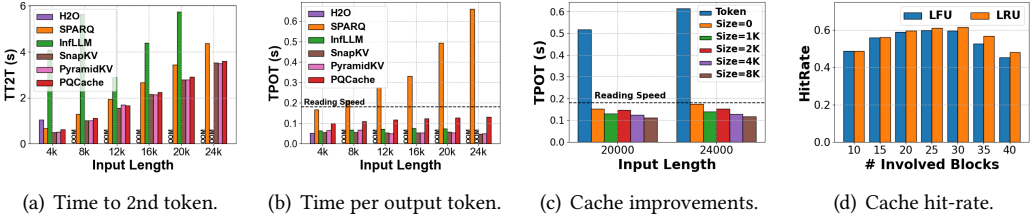


Fig. 11. (a-b) Latency experiments. (c-d) GPU Cache experiments.

**4.3.2 Cache Performance.** Based on the experiment settings of the previous section, we conduct an ablation study to evaluate the effectiveness of the GPU cache and assess the cache hit-rate. In Figure 11(c), we present the Time Per Output Token (TPOT) using various cache sizes ranging from 0 to 8K, including an experiment with a token-level cache of 4K size. Compared to the no-cache setting, the current block-level cache significantly reduces TPOT, decreasing time by 26.3% and 32.8% for 4K and 8K cache sizes, respectively. We don't utilize token-level cache, since it incurs high management overhead. We also plot the cache hit-rate for Least Recently Used (LRU) and Least Frequently Used (LFU) policies across different numbers of top- $k_{cache}$  blocks in Figure 11(d). This experiment is conducted on the HotpotQA dataset, with 1/10 tokens in selective attention and 4K tokens in GPU cache. Both LRU and LFU show similar performance, achieving around 0.5 hit-rate across different numbers of blocks. As the block count increases, the hit-rate initially rises because more tokens are found within blocks. However, it eventually declines as the block count exceeds the cache size, disrupting the cache update logic. In practice, we set the number of blocks to 32, matching the cache size and yielding a hit rate of approximately 0.6.

**4.3.3 Time Decomposition.** To verify our system improvements, we profile the time usage of LLM computation, PQ computation, and communication during both the prefilling and decoding phases. Figure 12(a) shows the profiled time of the prefilling phase. The KVCache offloading time is negligible compared to GPU computation and KMeans time, as the prefilling stage is compute-intensive with  $O(s^2)$  complexity. With the adaptive number of clustering iterations in PQCache, the KMeans computation time closely matches the GPU computation time, demonstrating the accuracy and effectiveness of our cost model. The end-to-end time for the entire prefilling phase, including GPU computation and KMeans, is also close to the GPU computation time due to perfect overlap of GPU computation, offloading, and KMeans processes.

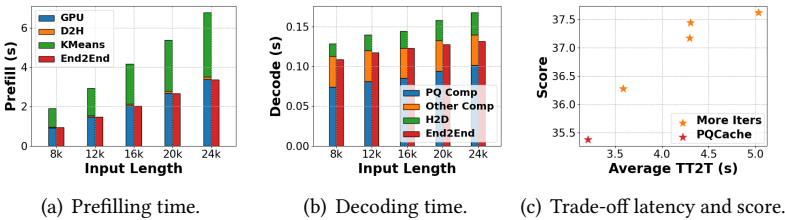


Fig. 12. (a-b) Time decomposition experiments. (c) HotpotQA performance with varying KMeans iterations.

Figure 12(b) shows the profiled time of the decoding phase. We decompose the decoding phase by profiling the PQ computation time (including top- $k$  token index time), LLM computation time,

and CPU-to-GPU communication time (including PQ codes and top- $k$  tokens' key-value pairs) without our GPU cache optimization. We also profile the end-to-end time with all optimizations. By using overlapping and GPU cache for acceleration, the PQ communication can be overlapped, and the token index time and top- $k$  tokens communication time can be reduced, resulting in an end-to-end time smaller than the sum of all components. Our decoding time remains stable with increasing input length.

**4.3.4 Number of Iterations in K-Means Clustering.** In PQCache, we design an adaptive K-Means clustering strategy to avoid blocking GPU computation. To investigate its impact on model accuracy, we conduct experiments with varying numbers of clustering iterations on the HotpotQA dataset, using Mistral-7B-inst-v0.2 and 1/10 of the tokens in attention. As shown in Figure 12(c), more clustering iterations generally improve accuracy but increase latency. Though the adaptive strategy has a relatively low score, it achieves the least Time To 2nd Token (TT2T) by not blocking GPU computation, and already performs well. Our experiments reveal the significant potential of integrating PQ into LLM inference, achieving superior performance when clustering is unrestricted. Additionally, PQCache offers flexibility to balance model quality and efficiency, providing practical options for various applications. For instance, in scenarios like mobile search, users may tolerate 7-10 seconds of latency<sup>4</sup>, but model performance is always crucial. We provide an interface that allows users to set the number of iterations, enabling them to balance model performance and latency according to their specific needs.

## 5 Discussion

**Hyper-parameter Tuning.** In PQCache, several hyperparameters require tuning. For the retrieval set size (top- $k$ ), intuitive and empirical evidence from previous subsections suggests that larger set sizes typically yield better performance. However, the practical limit is the available GPU memory. Practitioners should adjust this parameter based on their specific workloads and hardware capabilities. In the PQ settings, the number of iterations is automatically determined as detailed in Section 3.3. Tuning the number of clusters and segments is common and necessary in all PQ-based methods in both ANNS [44, 48] and deep learning scenarios [17, 101]. Here we provide a simple guideline for tuning. We suggest starting with the product of  $m$  and  $b$ , as it represents the size of the total vector space  $(2^b)^m = 2^{mb}$ . The optimal scale should be neither too small to compromise vector representation nor too large to overburden the clustering process. Once an optimal  $m \times b$  is found, minor adjustments can be made to refine the settings. As demonstrated in Section 4.2.7, performance varies slightly when maintaining a constant  $m \times b$ .

**Multiple Requests and Multiple GPUs.** PQCache can be directly applied to serve multiple requests. All computations and communications involved in PQCache, as detailed in Section 3, can be extended with a batch size dimension. The linear increase can be managed through parallel computation, thereby maximizing GPU utilization when a single request cannot fully utilize it. However, if the CPU is already compute-intensive, increasing the batch size might cause the CPU to block GPU computation. A simple solution is to add more CPUs, given their much lower cost compared to current GPUs. This solution is also applicable for multiple GPUs scenarios, where GPU computational capability is further enhanced.

**Longer Output Sequences and Multiple-turn Conversation.** At present, PQCache clusters once for PQ construction, which is suitable for most LLM inference scenarios with relatively short output sequences. We also assign new PQ codes to newly generated tokens based on their nearest centroids. However, in scenarios with longer outputs, input-based PQ structures may not capture

<sup>4</sup>Impact of Response Latency on User Behaviour in Mobile Web Search, Falk Scholer et al., CHIIR'21

new information from output tokens. A straightforward solution is to periodically reconstruct PQ to update the information. LLMs are also commonly used in multiple-turn conversations. In such cases, two strategies can be applied: (1) perform a prefill again upon each user input with all previous tokens; (2) perform K-Means on each input separately and add the output's PQ codes to the corresponding input. The choice of strategy can be tailored to the request, depending on whether the multiple turns are related.

**GPU and CPU Computational Capability.** In PQCache, model performance can sometimes be constrained by CPU computational capability, as we limit the number of clustering iterations on the CPU to prevent blocking GPU computation. In practice, LLM inference is often assigned to less computationally capable GPU cards, reserving more powerful cards for compute-intensive training. If the power of the GPU decreases, the K-Means clustering can have more iterations, which could potentially enhance the performance of PQCache in PQ construction. Therefore, PQCache is highly compatible with LLM inference. PQCache is ideally suited for environments with a proper GPU-to-CPU ratio, enabling effective PQ clustering to seamlessly overlap with LLM computation, regardless of whether the deployment is on the edge or in the cloud.

**Combined with LLM Inference/Serving Systems.** Several LLM inference/serving systems, including Orca [106], vLLM [51], and DistServe [115], have been proposed to enhance the overall efficiency. PQCache, which aims to use fewer tokens for attention, is orthogonal and compatible with these systems. As discussed in previous subsections, PQCache is compatible with batching techniques such as Orca [106]. vLLM [51]'s block-level PagedAttention can be seamlessly integrated into PQCache, also compatible with our block-level GPU cache. For systems like DistServe [115] that use prefill-decode disaggregation, PQCache only introduces new PQ structures communication, which is much smaller than the KVCache. While combining PQCache with these systems may require some engineering efforts, we anticipate the practical application of PQCache in contemporary LLM inference systems.

**Retrieval for LLM Inference.** To the best of our knowledge, our work is the first to incorporate information retrieval techniques into LLM inference. In LLM inference, especially in long-context scenarios, the generation of the next token naturally depends on relevant contexts, making the integration of retrieval techniques both intuitive and effective. We are proud to pioneer a new domain for efficient LLM inference and foresee the incorporation of retrieval as a standard paradigm in next-generation LLM inference. In PQCache, we currently utilize classic PQ structures for efficient LLM. Other retrieval techniques, such as IVF [48] and HNSW [62], along with recent advancements, could potentially contribute to more efficient LLM inference. We look forward to seeing more research exploring this new domain, leveraging and designing effective methods for improved LLM inference.

## 6 Related Work

**Selective Attention for KVCache.** To eliminate the impact of memory-intensive KVCache, a group of methods include only essential tokens for attention computation during LLM inference. One way is to discard unnecessary tokens. LM-Infinite [37] and Streaming-LLM [100] only preserve the initial tokens and the most recent tokens. H2O [112] and Scissorhands [59] utilize attention scores to identify important tokens. Their following works [2, 33, 77, 93] have explored adaptive token selection and additional metrics for better model accuracy. The LLMingua series [47, 70] leverage an auxiliary small model to tell which tokens are necessary. Since token-level compression evicts the tokens in a greedy manner, the information loss in subsequent decoding phase may lead to model degradation. Another way is to fetch relevant tokens on demand during the decoding phase.

SPARQ [79] and InfLLM [99] offload KVCache to CPU, and selectively fetch relevant key-value pairs for each attention computation. PQCache also falls under this category of methods, demonstrating effective and efficient LLM inference in comparison to existing techniques.

**KVCache Quantization.** Quantization can be directly applied on the entire KVCache [24, 38, 60] - a straight-forward approach with promising model quality. Other compression techniques can also be employed to address the residuals introduced by quantization [50]. Quantization is orthogonal to token importance, and recent research has explored applying both techniques [102].

**KVCache Scheduling.** Another related research direction is to meticulously schedule the KVCache within memory hierarchy. FlexGen [81] employs linear programming to schedule the communication, searching for efficient patterns to store and access tensors. AttentionScore [31] maintains a hierarchical KV caching system, allowing efficient reuse of KVCache across multi-turn conversations. KVCache streaming for LLM serving [58, 84] involves handling multiple requests within more levels of memory hierarchy.

**Embedding Management.** Embedding vector management is a common research focus within the database and data management domains, including embedding compression [82, 107, 110], embedding retrieval [41, 90], and key-value storage [19, 76]. Our work provides a potential direction for integrating classic embedding management methods into the LLM ecology.

## 7 Conclusion

In this paper, we proposed PQCache, a system-algorithm co-designed method for effective and efficient long context LLM inference. We incorporated the embedding retrieval technique PQ to reduce both memory and computation burden, and leveraged PQ codes and centroids to facilitate efficient ANN search for important tokens used in the attention module. Through meticulous overlapping and caching, we managed to minimize overhead to a negligible level. We evaluated PQCache through extensive experiments and showed that it improved model quality by 4.60% on InfiniteBench compared to existing methods, while maintaining low system latency.

## Acknowledgments

This work is supported by National Science and Technology Major Project (2022ZD0116315), National Natural Science Foundation of China (U23B2048, U22B2037, 62402011), Beijing Municipal Science and Technology Project (Z231100010323002), China National Postdoctoral Program for Innovative Talents (BX20230012), China Postdoctoral Science Foundation (2024M750103), Beijing Natural Science Foundation (4244080), research grant No. IPT-2024JK29, and High-performance Computing Platform of Peking University.

## References

- [1] Martin Abadi, Paul Barham, Jianmin Chen, Zhifeng Chen, Andy Davis, Jeffrey Dean, Matthieu Devin, Sanjay Ghemawat, Geoffrey Irving, Michael Isard, Manjunath Kudlur, Josh Levenberg, Rajat Monga, Sherry Moore, Derek Gordon Murray, Benoit Steiner, Paul A. Tucker, Vijay Vasudevan, Pete Warden, Martin Wicke, Yuan Yu, and Xiaoqiang Zheng. 2016. TensorFlow: A System for Large-Scale Machine Learning. In *12th USENIX Symposium on Operating Systems Design and Implementation, OSDI*.
- [2] Muhammad Adnan, Akhil Arunkumar, Gaurav Jain, Prashant J. Nair, Ilya Soloveychik, and Purushotham Kamath. 2024. Keyformer: KV Cache reduction through key tokens selection for Efficient Generative Inference. In *Proceedings of the Seventh Annual Conference on Machine Learning and Systems, MLSys*.
- [3] Moonshot AI. 2024. KimiChat. <https://kimi.moonshot.cn/>
- [4] Microsoft Research AI4Science and Microsoft Azure Quantum. 2023. The Impact of Large Language Models on Scientific Discovery: a Preliminary Study using GPT-4. *CoRR abs/2311.07361 (2023)*.

- [5] Fabien André, Anne-Marie Kermarrec, and Nicolas Le Scouarnec. 2015. Cache locality is not enough: High-Performance Nearest Neighbor Search with Product Quantization Fast Scan. *Proceedings of the VLDB Endowment* 9, 4 (2015), 288–299.
- [6] Anthropic. 2023. Long context prompting for Claude 2.1. <https://www.anthropic.com/news/claude-2-1-prompting>
- [7] Ilias Azizi. 2024. Vector Search on Billion-Scale Data Collections. *Proceedings of the VLDB Endowment*. ISSN 2150 (2024), 8097.
- [8] Ilias Azizi, Karima Echiabi, and Themis Palpanas. 2023. Elpis: Graph-Based Similarity Search for Scalable Data Science. *Proceedings of the VLDB Endowment* 16, 6 (2023), 1548–1559.
- [9] Shirram S. B, Anshuj Garg, and Purushottam Kulkarni. 2019. Dynamic Memory Management for GPU-Based Training of Deep Neural Networks. In *IEEE International Parallel and Distributed Processing Symposium, IPDPS*.
- [10] Yushi Bai, Xin Lv, Jiajie Zhang, Hongchang Lyu, Jiankai Tang, Zhidian Huang, Zhengxiao Du, Xiao Liu, Aohan Zeng, Lei Hou, Yuxiao Dong, Jie Tang, and Juanzi Li. 2024. LongBench: A Bilingual, Multitask Benchmark for Long Context Understanding. In *Proceedings of the 62nd Conference of the Association for Computational Linguistics (Volume 1: Long Papers), ACL*.
- [11] Dmitry Baranchuk, Artem Babenko, and Yury Malkov. 2018. Revisiting the Inverted Indices for Billion-Scale Approximate Nearest Neighbors. In *Computer Vision - ECCV - 15th European Conference*.
- [12] Kaifeng Bi, Lingxi Xie, Hengheng Zhang, Xin Chen, Xiaotao Gu, and Qi Tian. 2023. Accurate medium-range global weather forecasting with 3D neural networks. *Nature* 619, 7970 (2023), 533–538.
- [13] Rishi Bommasani, Drew A. Hudson, Ehsan Adeli, Russ B. Altman, Simran Arora, Sydney von Arx, Michael S. Bernstein, Jeannette Bohg, Antoine Bosselut, Emma Brunskill, Erik Brynjolfsson, Shyamal Buch, Dallas Card, Rodrigo Castellon, Niladri S. Chatterji, Annie S. Chen, Kathleen Creel, Jared Quincy Davis, Dorottya Demszky, Chris Donahue, Moussa Doumbouya, Esin Durmus, Stefano Ermon, John Etchemendy, Kawin Ethayarajah, Li Fei-Fei, Chelsea Finn, Trevor Gale, Lauren Gillespie, Karan Goel, Noah D. Goodman, Shelby Grossman, Neel Guha, Tatsunori Hashimoto, Peter Henderson, John Hewitt, Daniel E. Ho, Jenny Hong, Kyle Hsu, Jing Huang, Thomas Icard, Saahil Jain, Dan Jurafsky, Pratyusha Kalluri, Siddharth Karamcheti, Geoff Keeling, Fereshte Khani, Omar Khattab, Pang Wei Koh, Mark S. Krass, Ranjay Krishna, Rohith Kudipudi, and et al. 2021. On the Opportunities and Risks of Foundation Models. *CoRR* abs/2108.07258 (2021).
- [14] Zefan Cai, Yichi Zhang, Bofei Gao, Yuliang Liu, Tianyu Liu, Keming Lu, Wayne Xiong, Yue Dong, Baobao Chang, Junjie Hu, and Wen Xiao. 2024. PyramidKV: Dynamic KV Cache Compression based on Pyramidal Information Funneling. *CoRR* abs/2406.02069 (2024).
- [15] Abel Chandra, Laura Tünnermann, Tommy Löfstedt, and Regina Gratz. 2023. Transformer-based deep learning for predicting protein properties in the life sciences. *Elife* 12 (2023), e82819.
- [16] Qi Chen, Bing Zhao, Haidong Wang, Mingqin Li, Chuanjie Liu, Zengzhong Li, Mao Yang, and Jingdong Wang. 2021. SPANN: Highly-efficient Billion-scale Approximate Nearest Neighborhood Search. In *Advances in Neural Information Processing Systems, NeurIPS*.
- [17] Ting Chen, Lala Li, and Yizhou Sun. 2020. Differentiable Product Quantization for End-to-End Embedding Compression. In *International Conference on Machine Learning, ICML*.
- [18] Xiangping Chen, Xing Hu, Yuan Huang, He Jiang, Weixing Ji, Yanjie Jiang, Yanyan Jiang, Bo Liu, Hui Liu, Xiaochen Li, et al. 2025. Deep learning-based software engineering: progress, challenges, and opportunities. *Science China Information Sciences* 68, 1 (2025), 1–88.
- [19] Xubin Chen, Ning Zheng, Shukun Xu, Yifan Qiao, Yang Liu, Jiangpeng Li, and Tong Zhang. 2021. KallaxDB: A Table-less Hash-based Key-Value Store on Storage Hardware with Built-in Transparent Compression. In *Proceedings of the 17th International Workshop on Data Management on New Hardware, DaMoN*.
- [20] Alibaba Cloud. 2024. Tongyi Qianwen. <https://tongyi.aliyun.com/qianwen/>
- [21] Tri Dao. 2024. FlashAttention-2: Faster Attention with Better Parallelism and Work Partitioning. In *12th International Conference on Learning Representations, ICLR*.
- [22] Tri Dao, Daniel Y. Fu, Stefano Ermon, Atri Rudra, and Christopher Ré. 2022. FlashAttention: Fast and Memory-Efficient Exact Attention with IO-Awareness. In *Advances in Neural Information Processing Systems, NeurIPS*.
- [23] Harry Dong, Xinyu Yang, Zhenyu Zhang, Zhangyang Wang, Yuejie Chi, and Beidi Chen. 2024. Get More with LESS: Synthesizing Recurrence with KV Cache Compression for Efficient LLM Inference. In *International Conference on Machine Learning, ICML*.
- [24] Shichen Dong, Wen Cheng, Jiayu Qin, and Wei Wang. 2024. QAQ: Quality Adaptive Quantization for LLM KV Cache. *CoRR* abs/2403.04643 (2024).
- [25] Alexey Dosovitskiy, Lucas Beyer, Alexander Kolesnikov, Dirk Weissenborn, Xiaohua Zhai, Thomas Unterthiner, Mostafa Dehghani, Matthias Minderer, Georg Heigold, Sylvain Gelly, Jakob Uszkoreit, and Neil Houlsby. 2021. An Image is Worth 16x16 Words: Transformers for Image Recognition at Scale. In *9th International Conference on Learning Representations, ICLR*.

- [26] Abhimanyu Dubey, Abhinav Jauhri, Abhinav Pandey, Abhishek Kadian, Ahmad Al-Dahle, Aiesha Letman, Akhil Mathur, Alan Schelten, Amy Yang, Angela Fan, Anirudh Goyal, Anthony Hartshorn, Aobo Yang, Archi Mitra, Archie Sravankumar, Artem Korenev, Arthur Hinsvark, Arun Rao, Aston Zhang, Aurélien Rodriguez, Austen Gregerson, Ava Spataru, Baptiste Rozière, Bethany Biron, Binh Tang, Bobbie Chern, Charlotte Caucheteux, Chaya Nayak, Chloe Bi, Chris Marra, Chris McConnell, Christian Keller, Christophe Touret, Chunyang Wu, Corinne Wong, Cristian Canton Ferrer, Cyrus Nikolaidis, Damien Allonsius, Daniel Song, Danielle Pintz, Danny Livshits, David Esiobu, Dhruv Choudhary, Dhruv Mahajan, Diego Garcia-Olano, Diego Perino, Dieuwke Hupkes, Egor Lakomkin, Ehab AlBadawy, Elina Lobanova, Emily Dinan, Eric Michael Smith, Filip Radenovic, Frank Zhang, Gabriel Synnaeve, Gabrielle Lee, Georgia Lewis Anderson, Graeme Nail, Grégoire Mialon, Guan Pang, Guillem Cucurell, Hailey Nguyen, Hannah Korevaar, Hu Xu, Hugo Touvron, Iliyan Zarov, Imanol Arrieta Ibarra, Isabel M. Kloumann, Ishan Misra, Ivan Evtimov, Jade Copet, Jaewon Lee, Jan Geffert, Jana Vranes, Jason Park, Jay Mahadeokar, Jeet Shah, Jelmer van der Linde, Jennifer Billock, Jenny Hong, Jenya Lee, Jeremy Fu, Jianfeng Chi, Jianyu Huang, Jiawen Liu, Jie Wang, Jiecao Yu, Joanna Bitton, Joe Spisak, Jongsoo Park, Joseph Rocca, Joshua Johnstun, Joshua Saxe, Junteng Jia, Kalyan Vasuden Alwala, Kartikeya Upasani, Kate Plawiak, Ke Li, Kenneth Heafield, Kevin Stone, and et al. 2024. The Llama 3 Herd of Models. *CoRR* abs/2407.21783 (2024).
- [27] Ikraduya Edian. 2021. Accelerating Product Quantization Query Execution Runtime. In *International Conference on Management of Data, SIGMOD*.
- [28] Cong Fu, Chao Xiang, Changxu Wang, and Deng Cai. 2019. Fast Approximate Nearest Neighbor Search With The Navigating Spreading-out Graph. *Proceedings of the VLDB Endowment* 12, 5 (2019), 461–474.
- [29] Yao Fu, Litu Ou, Mingyu Chen, Yuhao Wan, Hao Peng, and Tushar Khot. 2023. Chain-of-Thought Hub: A Continuous Effort to Measure Large Language Models' Reasoning Performance. *CoRR* abs/2305.17306 (2023).
- [30] Yao Fu, Rameswar Panda, Xinyao Niu, Xiang Yue, Hannaneh Hajishirzi, Yoon Kim, and Hao Peng. 2024. Data Engineering for Scaling Language Models to 128K Context. In *International Conference on Machine Learning, ICML*.
- [31] Bin Gao, Zhuomin He, Puru Sharma, Qingxuan Kang, Djordje Jevdjic, Junbo Deng, Xingkun Yang, Zhou Yu, and Pengfei Zuo. 2024. AttentionStore: Cost-effective Attention Reuse across Multi-turn Conversations in Large Language Model Serving. *CoRR* abs/2403.19708 (2024).
- [32] Jianyang Gao and Cheng Long. 2024. RaBitQ: Quantizing High-Dimensional Vectors with a Theoretical Error Bound for Approximate Nearest Neighbor Search. In *International Conference on Management of Data, SIGMOD*.
- [33] Suyu Ge, Yunan Zhang, Liyuan Liu, Minjia Zhang, Jiawei Han, and Jianfeng Gao. 2024. Model Tells You What to Discard: Adaptive KV Cache Compression for LLMs. In *12th International Conference on Learning Representations, ICLR*.
- [34] Tiezheng Ge, Kaiming He, Qifa Ke, and Jian Sun. 2013. Optimized Product Quantization for Approximate Nearest Neighbor Search. In *IEEE Conference on Computer Vision and Pattern Recognition*.
- [35] Lei Guan, Dong-Sheng Li, Ji-Ye Liang, Wen-Jian Wang, Ke-Shi Ge, and Xi-Cheng Lu. 2024. Advances of pipeline model parallelism for deep learning training: an overview. *Journal of Computer Science and Technology* 39, 3 (2024), 567–584.
- [36] Sylvain Gugger, Lysandre Debut, Thomas Wolf, Philipp Schmid, Zachary Mueller, Sourab Mangrulkar, Marc Sun, and Benjamin Bossan. 2022. Accelerate: Training and inference at scale made simple, efficient and adaptable. <https://github.com/huggingface/accelerate>.
- [37] Chi Han, Qifan Wang, Wenhan Xiong, Yu Chen, Heng Ji, and Sinong Wang. 2023. LM-Infinite: Simple On-the-Fly Length Generalization for Large Language Models. *CoRR* abs/2308.16137 (2023).
- [38] Coleman Hooper, Sehoon Kim, Hiva Mohammadzadeh, Michael W. Mahoney, Yakun Sophia Shao, Kurt Keutzer, and Amir Gholami. 2024. KVQuant: Towards 10 Million Context Length LLM Inference with KV Cache Quantization. In *Advances in Neural Information Processing Systems, NeurIPS*.
- [39] Xinyi Hou, Yanjie Zhao, Yue Liu, Zhou Yang, Kailong Wang, Li Li, Xiapu Luo, David Lo, John Grundy, and Haoyu Wang. 2024. Large Language Models for Software Engineering: A Systematic Literature Review. *ACM Transactions on Software Engineering and Methodology* 33, 8 (2024), 220:1–220:79.
- [40] Qinghao Hu, Zhisheng Ye, Zerui Wang, Guoteng Wang, Meng Zhang, Qiaoling Chen, Peng Sun, Dahua Lin, Xiaolin Wang, Yingwei Luo, Yonggang Wen, and Tianwei Zhang. 2024. Characterization of Large Language Model Development in the Datacenter. In *21st USENIX Symposium on Networked Systems Design and Implementation, NSDI*.
- [41] Ruihong Huang, Shaoxu Song, Yunsu Lee, Jungho Park, Soo-Hyung Kim, and Sungmin Yi. 2020. Effective and Efficient Retrieval of Structured Entities. *Proceedings of the VLDB Endowment* 13, 6 (2020), 826–839.
- [42] Yanping Huang, Youlong Cheng, Ankur Bapna, Orhan Firat, Dehao Chen, Mia Xu Chen, HyoukJoong Lee, Jiquan Ngiam, Quoc V. Le, Yonghui Wu, and Zhifeng Chen. 2019. GPipe: Efficient Training of Giant Neural Networks using Pipeline Parallelism. In *Advances in Neural Information Processing Systems, NeurIPS*.
- [43] Suhas Jayaram Subramanya, Fnu Devvrit, Harsha Vardhan Simhadri, Ravishankar Krishnawamy, and Rohan Kadekodi. 2019. Diskann: Fast accurate billion-point nearest neighbor search on a single node. In *Advances in Neural Information*

*Processing Systems, NeurIPS.*

- [44] Hervé Jégou, Matthijs Douze, and Cordelia Schmid. 2011. Product Quantization for Nearest Neighbor Search. *IEEE Transactions on Pattern Analysis and Machine Intelligence* 33, 1 (2011), 117–128.
- [45] Albert Q. Jiang, Alexandre Sablayrolles, Arthur Mensch, Chris Bamford, Devendra Singh Chaplot, Diego de Las Casas, Florian Bressand, Gianna Lengyel, Guillaume Lample, Lucile Saulnier, Léo Renard Lavaud, Marie-Anne Lachaux, Pierre Stock, Teven Le Scao, Thibaut Lavril, Thomas Wang, Timothée Lacroix, and William El Sayed. 2023. Mistral 7B. *CoRR* abs/2310.06825 (2023).
- [46] Huiqiang Jiang, Yucheng Li, Chengruidong Zhang, Qianhui Wu, Xufang Luo, Surin Ahn, Zhenhua Han, Amir H. Abdi, Dongsheng Li, Chin-Yew Lin, Yuqing Yang, and Lili Qiu. 2024. MInference 1.0: Accelerating Pre-filling for Long-Context LLMs via Dynamic Sparse Attention. *CoRR* abs/2407.02490 (2024).
- [47] Huiqiang Jiang, Qianhui Wu, Chin-Yew Lin, Yuqing Yang, and Lili Qiu. 2023. LLMingua: Compressing Prompts for Accelerated Inference of Large Language Models. In *Proceedings of the Conference on Empirical Methods in Natural Language Processing, EMNLP*.
- [48] Jeff Johnson, Matthijs Douze, and Hervé Jégou. 2021. Billion-Scale Similarity Search with GPUs. *IEEE Transactions on Big Data* 7, 3 (2021), 535–547.
- [49] Greg Kamradt. 2024. Needle-in-a-Haystack. [https://github.com/gkamradt/LLMTest\\_NeedleInAHaystack](https://github.com/gkamradt/LLMTest_NeedleInAHaystack)
- [50] Hao Kang, Qingru Zhang, Souvik Kundu, Geonhwa Jeong, Zaoxing Liu, Tushar Krishna, and Tuo Zhao. 2024. GEAR: An Efficient KV Cache Compression Recipe for Near-Lossless Generative Inference of LLM. *CoRR* abs/2403.05527 (2024).
- [51] Woosuk Kwon, Zhuohan Li, Siyuan Zhuang, Ying Sheng, Lianmin Zheng, Cody Hao Yu, Joseph Gonzalez, Hao Zhang, and Ion Stoica. 2023. Efficient Memory Management for Large Language Model Serving with PagedAttention. In *Proceedings of the 29th Symposium on Operating Systems Principles, SOS*.
- [52] Yuhong Li, Yingbing Huang, Bowen Yang, Bharat Venkitesh, Acyr Locatelli, Hanchen Ye, Tianle Cai, Patrick Lewis, and Deming Chen. 2024. SnapKV: LLM Knows What You are Looking for Before Generation. *CoRR* abs/2404.14469 (2024).
- [53] Yinheng Li, Shaofei Wang, Han Ding, and Hang Chen. 2023. Large Language Models in Finance: A Survey. In *4th ACM International Conference on AI in Finance, ICAIF*.
- [54] Lucas D. Lingle. 2024. Transformer-VQ: Linear-Time Transformers via Vector Quantization. In *12th International Conference on Learning Representations, ICLR*.
- [55] Hao Liu, Wilson Yan, Matei Zaharia, and Pieter Abbeel. 2024. World Model on Million-Length Video And Language With Blockwise RingAttention. *CoRR* abs/2402.08268 (2024).
- [56] Jiesong Liu, Feng Zhang, Hourun Li, Dalin Wang, Weitao Wan, Xiaokun Fang, Jidong Zhai, and Xiaoyong Du. 2022. Exploring Query Processing on CPU-GPU Integrated Edge Device. *IEEE Transactions on Parallel and Distributed Systems* 33, 10 (2022), 4057–4070.
- [57] Yingfan Liu, Hong Cheng, and Jiangtao Cui. 2017. PQBF: I/O-Efficient Approximate Nearest Neighbor Search by Product Quantization. In *Proceedings of the Conference on Information and Knowledge Management, CIKM*.
- [58] Yuhan Liu, Hanchen Li, Yihua Cheng, Siddhant Ray, Yuyang Huang, Qizheng Zhang, Kuntai Du, Jiayi Yao, Shan Lu, Ganesh Ananthanarayanan, Michael Maire, Henry Hoffmann, Ari Holtzman, and Junchen Jiang. 2024. CacheGen: KV Cache Compression and Streaming for Fast Large Language Model Serving. In *Proceedings of the ACM SIGCOMM Conference*.
- [59] Zichang Liu, Aditya Desai, Fangshuo Liao, Weitao Wang, Victor Xie, Zhaozhuo Xu, Anastasios Kyrillidis, and Anshumali Shrivastava. 2023. Scissorhands: Exploiting the Persistence of Importance Hypothesis for LLM KV Cache Compression at Test Time. In *Advances in Neural Information Processing Systems, NeurIPS*.
- [60] Zirui Liu, Jiayi Yuan, Hongye Jin, Shaochen Zhong, Zhaozhuo Xu, Vladimir Braverman, Beidi Chen, and Xia Hu. 2024. KIVI: A Tuning-Free Asymmetric 2bit Quantization for KV Cache. In *International Conference on Machine Learning, ICML*.
- [61] Kejing Lu, Mineichi Kudo, Chuan Xiao, and Yoshiharu Ishikawa. 2021. HVS: Hierarchical Graph Structure Based on Voronoi Diagrams for Solving Approximate Nearest Neighbor Search. *Proceedings of the VLDB Endowment* 15, 2 (2021), 246–258.
- [62] Yury A. Malkov and Dmitry A. Yashunin. 2020. Efficient and Robust Approximate Nearest Neighbor Search Using Hierarchical Navigable Small World Graphs. *IEEE Transactions on Pattern Analysis and Machine Intelligence* 42, 4 (2020), 824–836.
- [63] Xupeng Miao, Xiaonan Nie, Hailin Zhang, Tong Zhao, and Bin Cui. 2023. Hetu: A highly efficient automatic parallel distributed deep learning system. *Science China Information Sciences* 66, 1 (2023), 117101.
- [64] Xupeng Miao, Gabriele Oliaro, Zhihao Zhang, Xinhao Cheng, Hongyi Jin, Tianqi Chen, and Zhihao Jia. 2023. Towards Efficient Generative Large Language Model Serving: A Survey from Algorithms to Systems. *CoRR* abs/2312.15234 (2023).

- [65] Sewon Min, Xinxi Lyu, Ari Holtzman, Mikel Artetxe, Mike Lewis, Hannaneh Hajishirzi, and Luke Zettlemoyer. 2022. Rethinking the Role of Demonstrations: What Makes In-Context Learning Work?. In *Proceedings of the Conference on Empirical Methods in Natural Language Processing, EMNLP*.
- [66] Shashi Narayan, Shay B. Cohen, and Mirella Lapata. 2018. Don't Give Me the Details, Just the Summary! Topic-Aware Convolutional Neural Networks for Extreme Summarization. In *Proceedings of the Conference on Empirical Methods in Natural Language Processing, EMNLP*.
- [67] Tung Nguyen, Johannes Brandstetter, Ashish Kapoor, Jayesh K. Gupta, and Aditya Grover. 2023. ClimaX: A foundation model for weather and climate. In *International Conference on Machine Learning, ICML*.
- [68] Xiaonan Nie, Xupeng Miao, Zhi Yang, and Bin Cui. 2022. TSPLIT: Fine-grained GPU Memory Management for Efficient DNN Training via Tensor Splitting. In *38th IEEE International Conference on Data Engineering, ICDE*.
- [69] OpenAI. 2023. GPT-4 Technical Report. *CoRR abs/2303.08774* (2023).
- [70] Zhuoshi Pan, Qianhui Wu, Huiqiang Jiang, Menglin Xia, Xufang Luo, Jue Zhang, Qingwei Lin, Victor Rühle, Yuqing Yang, Chin-Yew Lin, H. Vicky Zhao, Lili Qiu, and Dongmei Zhang. 2024. LLMingua-2: Data Distillation for Efficient and Faithful Task-Agnostic Prompt Compression. In *Findings of the Association for Computational Linguistics, ACL*.
- [71] Adam Paszke, Sam Gross, Francisco Massa, Adam Lerer, James Bradbury, Gregory Chanan, Trevor Killeen, Zeming Lin, Natalia Gimelshein, Luca Antiga, Alban Desmaison, Andreas Köpf, Edward Z. Yang, Zachary DeVito, Martin Raison, Alykhan Tejani, Sasank Chilamkurthy, Benoit Steiner, Lu Fang, Junjie Bai, and Soumith Chintala. 2019. PyTorch: An Imperative Style, High-Performance Deep Learning Library. In *Advances in Neural Information Processing Systems, NeurIPS*.
- [72] William Peebles and Saining Xie. 2023. Scalable Diffusion Models with Transformers. In *IEEE/CVF International Conference on Computer Vision, ICCV*.
- [73] Qwen Team. 2024. Qwen2.5: A Party of Foundation Models. <https://qwenlm.github.io/blog/qwen2.5/>
- [74] Samyam Rajbhandari, Olatunji Ruwase, Jeff Rasley, Shaden Smith, and Yuxiong He. 2021. ZeRO-infinity: breaking the GPU memory wall for extreme scale deep learning. In *International Conference for High Performance Computing, Networking, Storage and Analysis, SC*.
- [75] Jie Ren, Samyam Rajbhandari, Reza Yazdani Aminabadi, Olatunji Ruwase, Shuangyan Yang, Minjia Zhang, Dong Li, and Yuxiong He. 2021. ZeRO-Offload: Democratizing Billion-Scale Model Training. In *USENIX Annual Technical Conference, ATC*.
- [76] Kai Ren, Qing Zheng, Joy Arulraj, and Garth Gibson. 2017. SlimDB: A Space-Efficient Key-Value Storage Engine For Semi-Sorted Data. *Proceedings of the VLDB Endowment* 10, 13 (2017), 2037–2048.
- [77] Siyu Ren and Kenny Q. Zhu. 2024. On the Efficacy of Eviction Policy for Key-Value Constrained Generative Language Model Inference. *CoRR abs/2402.06262* (2024).
- [78] Minsoo Rhu, Natalia Gimelshein, Jason Clemons, Arslan Zulfiqar, and Stephen W. Keckler. 2016. vDNN: Virtualized deep neural networks for scalable, memory-efficient neural network design. In *49th Annual IEEE/ACM International Symposium on Microarchitecture, MICRO*.
- [79] Luka Ribar, Ivan Chelombiev, Luke Hudlass-Galley, Charlie Blake, Carlo Luschi, and Douglas Orr. 2024. SparQ Attention: Bandwidth-Efficient LLM Inference. In *International Conference on Machine Learning, ICML*.
- [80] Ludan Ruan and Qin Jin. 2022. Survey: Transformer based video-language pre-training. *AI Open* 3 (2022), 1–13.
- [81] Ying Sheng, Lianmin Zheng, Binhang Yuan, Zhuohan Li, Max Ryabinin, Beidi Chen, Percy Liang, Christopher Ré, Ion Stoica, and Ce Zhang. 2023. FlexGen: High-Throughput Generative Inference of Large Language Models with a Single GPU. In *International Conference on Machine Learning, ICML*.
- [82] Hao-Jun Michael Shi, Dheevatsa Mudigere, Maxim Naumov, and Jiyan Yang. 2020. Compositional Embeddings Using Complementary Partitions for Memory-Efficient Recommendation Systems. In *The 26th ACM SIGKDD Conference on Knowledge Discovery and Data Mining*.
- [83] Yuan-Feng Song, Yuan-Qin He, Xue-Fang Zhao, Han-Lin Gu, Di Jiang, Hai-Jun Yang, and Li-Xin Fan. 2024. A communication theory perspective on prompting engineering methods for large language models. *Journal of Computer Science and Technology* 39, 4 (2024), 984–1004.
- [84] Foteini Strati, Sara McAllister, Amar Phanishayee, Jakub Tarnawski, and Ana Klimovic. 2024. DéjàVu: KV-cache Streaming for Fast, Fault-tolerant Generative LLM Serving. In *International Conference on Machine Learning, ICML*.
- [85] Hanlin Tang, Yang Lin, Jing Lin, Qingsen Han, Shikuan Hong, Yiwu Yao, and Gongyi Wang. 2024. RazorAttention: Efficient KV Cache Compression Through Retrieval Heads. *CoRR abs/2407.15891* (2024).
- [86] Rohan Taori, Ishaan Gulrajani, Tianyi Zhang, Yann Dubois, Xuechen Li, Carlos Guestrin, Percy Liang, and Tatsunori B Hashimoto. 2023. Alpaca: A strong, replicable instruction-following model. *Stanford Center for Research on Foundation Models* 3, 6 (2023), 7.
- [87] Together.ai. 2023. LLaMA-2-7B-32K. <https://huggingface.co/togethercomputer/LLaMA-2-7B-32K>
- [88] Hugo Touvron, Louis Martin, Kevin Stone, Peter Albert, Amjad Almahairi, Yasmine Babaei, Nikolay Bashlykov, Soumya Batra, Prajjwal Bhargava, Shrutvi Bhosale, Dan Bikel, Lukas Blecher, Cristian Canton-Ferrer, Moya Chen,

- Guillem Cucurull, David Esioju, Jude Fernandes, Jeremy Fu, Wenyin Fu, Brian Fuller, Cynthia Gao, Vedanuj Goswami, Naman Goyal, Anthony Hartshorn, Saghar Hosseini, Rui Hou, Hakan Inan, Marcin Kardas, Viktor Kerkez, Madian Khabsa, Isabel Kloumann, Artem Korenev, Punit Singh Koura, Marie-Anne Lachaux, Thibaut Lavril, Jenya Lee, Diana Liskovich, Yinghai Lu, Yuning Mao, Xavier Martinet, Todor Mihaylov, Pushkar Mishra, Igor Molybog, Yixin Nie, Andrew Poulton, Jeremy Reizenstein, Rashi Rungta, Kalyan Saladi, Alan Schelten, Ruan Silva, Eric Michael Smith, Ranjan Subramanian, Xiaoqing Ellen Tan, Binh Tang, Ross Taylor, Adina Williams, Jian Xiang Kuan, Puxin Xu, Zheng Yan, Iliyan Zarov, Yuchen Zhang, Angela Fan, Melanie Kambadur, Sharan Narang, Aurélien Rodriguez, Robert Stojnic, Sergey Edunov, and Thomas Scialom. 2023. Llama 2: Open Foundation and Fine-Tuned Chat Models. *CoRR abs/2307.09288* (2023).
- [89] Aäron van den Oord, Oriol Vinyals, and Koray Kavukcuoglu. 2017. Neural Discrete Representation Learning. In *Advances in Neural Information Processing Systems, NeurIPS*.
- [90] Mengzhao Wang, Xiaoliang Xu, Qiang Yue, and Yuxiang Wang. 2021. A Comprehensive Survey and Experimental Comparison of Graph-Based Approximate Nearest Neighbor Search. *Proceedings of the VLDB Endowment* 14, 11 (2021), 1964–1978.
- [91] Runhui Wang and Dong Deng. 2020. DeltaPQ: Lossless Product Quantization Code Compression for High Dimensional Similarity Search. *Proceedings of the VLDB Endowment* 13, 13 (2020), 3603–3616.
- [92] Xiaofei Wang, Yiwen Han, Victor C. M. Leung, Dusit Niyato, Xueqiang Yan, and Xu Chen. 2020. Convergence of Edge Computing and Deep Learning: A Comprehensive Survey. *IEEE Communications Surveys and Tutorials* 22, 2 (2020), 869–904.
- [93] Zihao Wang, Bin Cui, and Shaoduo Gan. 2024. SqueezeAttention: 2D Management of KV-Cache in LLM Inference via Layer-wise Optimal Budget. *CoRR abs/2404.04793* (2024).
- [94] Jason Wei, Xuezhi Wang, Dale Schuurmans, Maarten Bosma, Brian Ichter, Fei Xia, Ed H. Chi, Quoc V. Le, and Denny Zhou. 2022. Chain-of-Thought Prompting Elicits Reasoning in Large Language Models. In *Advances in Neural Information Processing Systems, NeurIPS*.
- [95] Qizhen Weng, Wencong Xiao, Yinghao Yu, Wei Wang, Cheng Wang, Jian He, Yong Li, Liping Zhang, Wei Lin, and Yu Ding. 2022. MLaaS in the Wild: Workload Analysis and Scheduling in Large-Scale Heterogeneous GPU Clusters. In *19th USENIX Symposium on Networked Systems Design and Implementation, NSDI*.
- [96] Manuel Widmoser, Daniel Kocher, and Nikolaus Augsten. 2024. Scalable Distributed Inverted List Indexes in Disaggregated Memory. In *International Conference on Management of Data, SIGMOD*.
- [97] Bingyang Wu, Zili Zhang, Zhihao Bai, Xuanzhe Liu, and Xin Jin. 2023. Transparent GPU Sharing in Container Clouds for Deep Learning Workloads. In *20th USENIX Symposium on Networked Systems Design and Implementation, NSDI*.
- [98] Likang Wu, Zhi Zheng, Zhaopeng Qiu, Hao Wang, Hongchao Gu, Tingjia Shen, Chuan Qin, Chen Zhu, Hengshu Zhu, Qi Liu, Hui Xiong, and Enhong Chen. 2024. A survey on large language models for recommendation. *World Wide Web (WWW)* 27, 5 (2024), 60.
- [99] Chaojun Xiao, Pengle Zhang, Xu Han, Guangxuan Xiao, Yankai Lin, Zhengyan Zhang, Zhiyuan Liu, Song Han, and Maosong Sun. 2024. InFLM: Unveiling the Intrinsic Capacity of LLMs for Understanding Extremely Long Sequences with Training-Free Memory. *CoRR abs/2402.04617* (2024).
- [100] Guangxuan Xiao, Yuandong Tian, Beidi Chen, Song Han, and Mike Lewis. 2024. Efficient Streaming Language Models with Attention Sinks. In *12th International Conference on Learning Representations, ICLR*.
- [101] Shitao Xiao, Zheng Liu, Weihao Han, Jianjin Zhang, Defu Lian, Yeyun Gong, Qi Chen, Fan Yang, Hao Sun, Yingxia Shao, and Xing Xie. 2022. Distill-VQ: Learning Retrieval Oriented Vector Quantization By Distilling Knowledge from Dense Embeddings. In *The 45th International ACM SIGIR Conference on Research and Development in Information Retrieval*.
- [102] June Yong Yang, Byeongwook Kim, Jeongin Bae, Beomseok Kwon, Gunho Park, Eunho Yang, Se Jung Kwon, and Dongsoo Lee. 2024. No Token Left Behind: Reliable KV Cache Compression via Importance-Aware Mixed Precision Quantization. *CoRR abs/2402.18096* (2024).
- [103] Rui Yang, Ting Fang Tan, Wei Lu, Arun James Thirunavukarasu, Daniel Shu Wei Ting, and Nan Liu. 2023. Large language models in health care: Development, applications, and challenges. *Health Care Science* 2, 4 (2023), 255–263.
- [104] Wen Yang, Tao Li, Gai Fang, and Hong Wei. 2020. PASE: PostgreSQL Ultra-High-Dimensional Approximate Nearest Neighbor Search Extension. In *International Conference on Management of Data, SIGMOD*.
- [105] Zhisheng Ye, Wei Gao, Qinghao Hu, Peng Sun, Xiaolin Wang, Yingwei Luo, Tianwei Zhang, and Yonggang Wen. 2024. Deep Learning Workload Scheduling in GPU Datacenters: A Survey. *Comput. Surveys* 56, 6 (2024), 146:1–146:38.
- [106] Gyeong-In Yu, Joo Seong Jeong, Geon-Woo Kim, Soojeong Kim, and Byung-Gon Chun. 2022. Orca: A Distributed Serving System for Transformer-Based Generative Models. In *16th USENIX Symposium on Operating Systems Design and Implementation, OSDI*.
- [107] Hailin Zhang, Zirui Liu, Boxuan Chen, Yikai Zhao, Tong Zhao, Tong Yang, and Bin Cui. 2024. CAFE: Towards Compact, Adaptive, and Fast Embedding for Large-scale Recommendation Models. In *International Conference on*

*Management of Data, SIGMOD.*

- [108] Hailin Zhang, Yujing Wang, Qi Chen, Ruiheng Chang, Ting Zhang, Ziming Miao, Yingyan Hou, Yang Ding, Xupeng Miao, Haonan Wang, Bochen Pang, Yuefeng Zhan, Hao Sun, Weiwei Deng, Qi Zhang, Fan Yang, Xing Xie, Mao Yang, and Bin Cui. 2023. Model-enhanced Vector Index. In *Advances in Neural Information Processing Systems, NeurIPS*.
- [109] Huangzhao Zhang, Kechi Zhang, Zhuo Li, Jia Li, Jia Li, Yongmin Li, Yunfei Zhao, Yuqi Zhu, Fang Liu, Ge Li, et al. 2024. Deep learning for code generation: a survey. *Science China Information Sciences* 67, 9 (2024), 191101.
- [110] Hailin Zhang, Penghao Zhao, Xupeng Miao, Yingxia Shao, Zirui Liu, Tong Yang, and Bin Cui. 2023. Experimental Analysis of Large-scale Learnable Vector Storage Compression. *Proceedings of the VLDB Endowment* 17, 4 (2023), 808–822.
- [111] Xinrong Zhang, Yingfa Chen, Shengding Hu, Zihang Xu, Junhao Chen, Moo Hao, Xu Han, Zhen Thai, Shuo Wang, Zhiyuan Liu, and Maosong Sun. 2024.  $\infty$ Bench: Extending Long Context Evaluation Beyond 100K Tokens. In *Proceedings of the 62nd Conference of the Association for Computational Linguistics (Volume 1: Long Papers), ACL*.
- [112] Zhenyu Zhang, Ying Sheng, Tianyi Zhou, Tianlong Chen, Lianmin Zheng, Ruisi Cai, Zhao Song, Yuandong Tian, Christopher Ré, Clark W. Barrett, Zhangyang Wang, and Beidi Chen. 2023. H2O: Heavy-Hitter Oracle for Efficient Generative Inference of Large Language Models. In *Advances in Neural Information Processing Systems, NeurIPS*.
- [113] Xi Zhao, Yao Tian, Kai Huang, Bolong Zheng, and Xiaofang Zhou. 2023. Towards Efficient Index Construction and Approximate Nearest Neighbor Search in High-Dimensional Spaces. *Proceedings of the VLDB Endowment* 16, 8 (2023), 1979–1991.
- [114] Zangwei Zheng, Xiangyu Peng, Tianji Yang, Chenhui Shen, Shenggui Li, Hongxin Liu, Yukun Zhou, Tianyi Li, and Yang You. 2024. Open-Sora: Democratizing Efficient Video Production for All. *CoRR* abs/2412.20404 (2024).
- [115] Yinmin Zhong, Shengyu Liu, Junda Chen, Jianbo Hu, Yibo Zhu, Xuanzhe Liu, Xin Jin, and Hao Zhang. 2024. Dist-Serve: Disaggregating Prefill and Decoding for Goodput-optimized Large Language Model Serving. In *18th USENIX Symposium on Operating Systems Design and Implementation, OSDI*.
- [116] Jingbo Zhou, Qi Guo, H. V. Jagadish, Lubos Krcál, Siyuan Liu, Wenhao Luan, Anthony K. H. Tung, Yueji Yang, and Yuxin Zheng. 2018. A Generic Inverted Index Framework for Similarity Search on the GPU. In *34th IEEE International Conference on Data Engineering, ICDE*.
- [117] Xuanhe Zhou, Zhaoyan Sun, and Guoliang Li. 2024. Db-gpt: Large language model meets database. *Data Science and Engineering* 9, 1 (2024), 102–111.
- [118] Jingyu Zhu, Xintong Zhao, Yu Sun, Shaouxu Song, and Xiaojie Yuan. 2024. Relational Data Cleaning Meets Artificial Intelligence: A Survey. *Data Science and Engineering* (2024), 1–28.

Received October 2024; revised January 2025; accepted February 2025